Ga2O3/Al2O3 Catalysts for Propane Dehydrogenation: Modification of Surface Properties by H2 pretreatment or co-feeding

Sebastian Amar Gil, Catherine Especel, Francisco Passamonti, V. Montouillout, Viviana Benítez, Florence Epron

Ga_2O_3/Al_2O_3 CATALYSTS FOR PROPANE DEHYDROGENATION: EFFECT OF H_2 TREATMENT AND CO-FEEDING

Sebastian Amar Gil,*[a] Catherine Especel,[a] Francisco J. Passamonti,[b] Valérie Montouillout,[c] Viviana M. Benítez,*[b] Florence Epron*[a]

[a] S. Amar Gil, C. Especel, F. Epron
CNRS, Université de Poitiers, Institut de Chimie des Milieux et Matériaux de Poitiers-IC2MP, Poitiers, France
E-mail: florence.epron@univ-poitiers.fr, sebastian.amar.gil@univ-poitiers.fr

[b] F. J. Passamonti, V. M. Benítez
Instituto de Investigaciones en Catálisis y Petroquímica - INCAPE
Universidad Nacional del Litoral
Colectora Ruta Nac. Nº 168 Km. 0 - Paraje El Pozo, 3000 Santa Fe, Argentina
E-mail: vbenitez@fiq.unl.edu.ar

[c] V. Montouillout
Conditions Extrêmes et Matériaux: Haute Température et Irradiation, CEMHTI, UPR 3079 -CNRS Univ Orléans, Orléans, France

Abstract: This study investigated the catalytic dehydrogenation of propane over uncalcined, calcined or pre-reduced gallium-supported alumina catalysts. The effects induced by a reductive pretreatment and hydrogen co-feeding (5 % and 50 % in volume in the gas mixture) on the catalytic performance were evaluated. For comparison, a non-supported γ-Ga_2O_3 sample was prepared. The catalysts were characterized by different methods including XRD, TEM, SEM, NMR, TPR, FTIR, pyridine-FTIR and the model reaction of 3,3-dimethylbut-1-ene isomerization. It was found that reductive pretreatment improved the propylene production in gas phase but decreased the initial conversion compared to the calcined sample. Hydrogen co-feeding positively impacted the catalytic stability of reduced catalysts, leading to a higher conversion after 240 min and reducing the deactivation of the catalyst up to 70 % as the amount of H_2 increased in the stream. Moreover, improvement in the carbon balance and reduction of carbon deposited were observed at high H_2 co-feeding ratio. The formation of gallium hydride species during the reduction pretreatment and H_2 flowing was clearly identified, but their contribution in the PDH reaction can be considered as negligible compared to positive effect induced by the decrease in acidity due to the reducing pretreatment.

Introduction

Propylene is a crucial basic chemical for the production of a diverse range of chemicals, including polypropylene, acrolein, and polyacrylonitrile, and the market demand of this chemical compound has seen a notable increase in recent years.[1] Propylene is primarily obtained as a by-product from naphtha steam crackers and fluidized catalytic cracking (FCC) units in refineries.[2] These conventional methods yield a relative limited amount of propylene, around 15 – 20 % for steam crackers and 5% for FCC processes, and they are coupled with ethylene production.[3] In recent years, the gap between demand and supply of propylene has grown, due to the market increase and economic interest.[2,4] On-purpose technologies, such as catalytic propane dehydrogenation (PDH), have drawn attention as alternative methods for propylene production.[5,6] While PDH technology demonstrates notable economic performance, challenges such as the high cost, rapid coking, deep dehydrogenation and sintering on Pt-based and CrO_x-based catalysts, are not enough to satisfy the current demand.[1,7] Therefore, developing an alternative to these two commercial catalysts has been stimulated in both industry and academia.[8]

Hence, many oxides such as Ga_2O_3,[9] VO_x,[10] ZrO_2,[11] and ZnO[12] have been extensively studied for PDH, among which Ga_2O_3 is a very promising candidate, since it presents low toxicity, thermal stability and low cost of synthesis.[13] While Ga_2O_3 deactivates quickly,[14] recent reports have demonstrated that Ga_2O_3 deposited on various oxide supports, such as SiO_2,[9,15] Al_2O_3,[16,17] and ZrO_2,[18,19] can be more active and stable. Supported Ga_2O_3 catalysts are typically prepared by incipient wetness impregnation of $Ga(NO_3)_3$ aqueous solution onto oxide supports followed by calcination, although practically, the nitrate route may yield a broad distribution of active sites.[9] Especially, Al_2O_3-supported Ga catalysts have shown promising selectivity.[17]

On Ga_2O_3/SiO_2, Castro-Fernández and co-workers reported that the catalyst with the highest fraction of β-Ga_2O_3 is more active in PDH than the γ-rich Ga_2O_3 catalyst due to the higher proportion of weak Lewis acidic sites (LAS) in β-Ga_2O_3,

since γ-Ga_2O_3 lacks these sites.[9,14] Likewise, tetracoordinated Ga^{3+} LAS (Ga_{IV}) were proposed as active sites for PDH on Ga_2O_3-based catalysts.[9] These authors proposed that there is a larger fraction of weaker LAS in β-Ga_2O_3 relative to γ-Ga_2O_3. Since β-Ga_2O_3 has notably higher catalytic activity in PDH in comparison to γ-Ga_2O_3 and α-Ga_2O_3, weak LAS are proposed to drive propene formation during propane dehydrogenation. Also, it has been demonstrated that Ga-hydrides are formed in the presence of the hydrogen produced during PDH, which may play a negative role on the reaction rate and the yield in propylene.[15] H_2 dissociates onto the Ga^{3+}-O sites, which are also the active sites for propane heterolytic C-H cleavage, yielding Ga^{3+}H-OH sites that are inactive for PDH. Weaker LAS are expected to give weaker-bonded gallium hydrides, desorbing H_2 more efficiently. Therefore, Ga^{3+}-O sites are more readily recovered for the PDH cycle.[20]

In order to study the effect of hydrogen on the catalytic properties, two ways are generally studied in the literature either by introducing H_2 during the pretreatment step or by co-feeding H_2 during the catalytic test. The first method consists of pretreating the calcined catalyst under H_2 at high temperature, then purging under inert gas before starting the catalytic test in the absence of hydrogen flowing.[15,21,22] According to Liu and co-workers, Ga- H_x species are formed on Ga_2O_3/SiO_2 under high temperature H_2 pretreatment by heterolytic dissociation of dihydrogen on Ga-O dual sites.[15] These hydride species, detrimental to the catalytic performance, are removed during time-on-stream when the catalytic test of PDH is performed under 5 vol% C_3H_8/N_2, leading to an increase in propylene production.[15] Castro-Fernández and co-workers demonstrated that, on unsupported nanocrystalline Ga_2O_3 nanoparticles, H_2 pretreatment at 500 °C leads, for both γ-Ga_2O_3 and β-Ga_2O_3, to the formation of vacancies and gallium hydrides, to a modification of the LAS distribution and to a surface reconstruction.[14] This reconstruction increases the density of surface Ga sites associated with a higher activity in the PDH reaction for H_2-treated γ-Ga_2O_3. On β-Ga_2O_3, the reduction treatment increases the proportion of weak acid sites, thus increasing the activity. Consequently, the effect of the pretreatment strongly depends on the type of gallium oxides. On GaO_x/Al_2O_3, Sun and co-workers observed that the pre-reduction at 600 °C increases the initial conversion and propene selectivity.[23] It was proposed by these authors that gallium oxide is partially reduced to $Ga^{\delta+}O_x$ species, with $\delta < 3$ with roughly 25 % of the surface gallium species in the form of $Ga^{\delta+}$.

The effect of H_2 on the gallium speciation and on the catalytic performance can also be studied by using H_2 co-feeding during the catalytic test. In that case, catalysts were either used calcined, *i.e.* heated up to the reaction temperature under inert gas, or pre-treated under H_2 at high temperature, before the catalytic test performed with co-feeding hydrogen.[23,24] Zhou and co-workers studied the effect of H_2 co-feeding on calcined Ga_2O_3/Al_2O_3 catalysts.[24] The addition of H_2 to the gas stream favors the formation of GaH_x species, which has a positive effect on the initial propane conversion, avoids the decrease in selectivity to propene as a function of time-on-stream, and limits coke deposition. It was proposed by Sun and co-workers that these gallium hydrides species are formed by homolytic dissociation on partially reduced adjacent coordinatively unsaturated (cus) gallium atoms displayed on the pre-reduced GaO_x/Al_2O_3 catalyst.[23] These gallium hydride species are metastable and are not observed in the absence of H_2 co-feeding. The catalytic performances were correlated with the surface coverage of gallium hydride species, which promotes the C-H bond activation and limits deep dehydrogenation.[23]

All these results obtained by pretreating Ga_2O_3 catalysts alone or supported on different oxides under hydrogen, or by adding hydrogen to the gas stream, produce sometimes opposite results. It is possible that the pre-reduction leads to a partial reduction of gallium oxides and changes their dispersion. However, there is no consensus on the impact of hydride species on catalytic properties. For some, even in the absence of co-feeding, hydrides would be present and have a negative impact on the PDH reaction, while for others, hydrides would be metastable, and their presence would require H_2 co-feeding, leading to improved catalytic properties. More importantly, for alumina supported GaO_x catalysts, although special attention was paid to the characterization of hydride species and the state of Ga species after reduction, to our knowledge, the acidity of the catalysts was always characterized before reduction, whereas acidity is also an important parameter for catalytic performance that may change after a reductive pre-treatment. It would therefore seem that the pre-treatment conditions, the nature of the support and of the interactions between the support and gallium, as well as test conditions have different impacts that need to be rationalized. In the present work, a systematic study of the effects of H_2 co-feeding on Ga_2O_3/Al_2O_3 catalysts calcined or pre-reduced is proposed. Calcination of catalysts after impregnation favors metal-support interactions and may play an important role in gallium dispersion and in its reducibility. Therefore, in order to vary these interactions, two starting materials will be studied, namely calcined and non-calcined catalysts, as well as a non-supported γ-Ga_2O_3 catalyst, that will be activated by pre-treatment either under N_2 or H_2 before catalytic test. All catalysts will be thoroughly characterized, especially the acidity and hydride formation according to the pretreatments performed.

Results and Discussion

Physical and chemical properties of the support and catalysts

Ga_2O_3/Al_2O_3 catalysts were characterized after impregnation of the precursor salt on the alumina support, and drying (Ga/Al_d) and then after calcination (Ga/Al), and compared with the Al_2O_3 and Ga_2O_3 oxides. The content of gallium in the supported catalysts was characterized by ICP-OES, getting a weight loading very close to the nominal one (5 wt.%, Table 1). The pore size, pore volume and BET surface area were determined based on N_2-sorption isotherms at 77 K. In all the cases, the materials present a type IV isotherm (Figure S1), typical of mesoporous materials.[16] The profiles of the pore size distribution show that γ-Al_2O_3 support and Ga/Al, Ga/Al_d catalysts present a narrow pore size distribution. The BET surface areas, the pore diameters, and the total pore volumes of the catalysts were calculated and the results are shown in Table 1. The BET surface area of the gallia sample is about 122 $m^2\ g^{-1}$ and the alumina support and supported catalysts exhibited a similar surface area, around 192 $m^2\ g^{-1}$ regardless the material, indicating that the deposition of Ga has no effect on the textural properties of the alumina support, even after calcination. The average pore diameter is of 10.6, 10.8 and 8.5 nm for Al_2O_3, Ga/Al and Ga/Al_d samples, respectively, the Ga_2O_3 sample presents an average pore diameter of 6.2 nm.

Table 1. Textural properties and Ga content of γ-Al_2O_3, γ-Ga_2O_3, Ga/Al and Ga/Al_d catalysts.

Catalyst	Ga (wt.%)[a]	S_{BET} ($m^2\ g^{-1}$)	V_{total} ($cm^3\ g^{-1}$)	Dp (nm)[b]
γ-Ga_2O_3	74.3	122	0.19	6.2
γ-Al_2O_3	-	196	0.52	10.6
Ga/Al	4.9	189	0.51	10.8
Ga/Al_d	4.8	194	0.41	8.5

[a] Determined by ICP-OES. [b] Calculated as $4V_{total}/S_{BET}$.

The XRD patterns of pure γ-Ga_2O_3, γ-Al_2O_3, Ga/Al and Ga/Al_d samples are presented in Figure 1. For the alumina support alone, all diffraction lines, located at 37.1 °, 45.7 ° and 66.7 °, are typical of γ-Al_2O_3 phase; they are broad due to the low crystallinity of the sample probably due to the high surface area of this material.[25] The XRD pattern of the unsupported Ga_2O_3 is typical of γ-Ga_2O_3 phase, in accordance with what is expected given the synthesis method.[26,27] Diffraction lines are broader than that of γ-Al_2O_3 support, showing the lower crystallinity of this sample. Moreover, no diffraction line assigned to other Ga_2O_3 polymorphs was observed on the gallium oxide sample (e.g., α-, β-, and δ-Ga_2O_3). However, it cannot be excluded that these phases are also present in this sample. For Ga/Al and Ga/Al_d catalysts, the XRD pattern corresponds to that of the bare γ-Al_2O_3 support, with no diffraction peak corresponding to Ga_2O_3 phase indicating that no matter the thermal treatment after Ga deposition, gallium species apparently do not modify the alumina structure. The absence of diffraction lines corresponding to gallium oxides indicates that, whatever the type of gallium species displayed after calcination or drying they may be highly dispersed at the surface of the alumina support. To check if gallium atoms could be inserted in the alumina framework the unit cell parameter was estimated from the 2θ position of the (044) reflection. The same value than for Al_2O_3 (0.791 nm) was obtained for the two samples (Ga/Al and Ga/Al_d). This can be due to the small quantity of Ga in the samples (*c.a.* atomic ratio Ga:Al = 1:26). Even if the insertion of gallium species in the Al_2O_3 framework should be limited to the surface of the alumina support, after the thermal pre-treatment under air or N_2 at high temperature, given the catalyst surface area, the gallium loading and the proportion of surface Al^{3+} sites of γ-Al_2O_3 (14.5 $Al^{3+}\ nm^{-2}$), a maximum of 2 Ga^{3+} per nm^2 can be present at the surface.[28] If Ga^{3+} is inserted by replacement of Al^{3+} in the framework, this will give 2 Ga^{3+} for 12.5 Al^{3+} per nm^2 and an atomic ratio Ga:Al of *ca.*1:6. in surface.

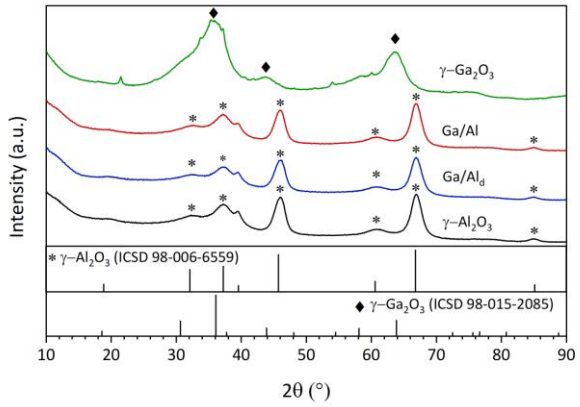

Figure 1. XRD patterns of γ-Ga_2O_3, γ-Al_2O_3, Ga/Al, Ga/Al_d catalysts and γ-Ga_2O_3, γ-Al_2O_3 references.

To check if gallium atoms can be inserted in the Al_2O_3 framework after thermal treatment, high resolution solid state nuclear magnetic resonance spectroscopy (NMR) was performed on the on the γ-Al_2O_3, Ga/Al and Ga/Al_{d_N2} (treated under N_2 at 575°C) samples. Results are presented in Figure 2. In both Ga/Al and Ga/Al_{d_N2} cases, the ^{71}Ga MAS NMR spectra are composed of two resonances with broad asymmetric line shapes due to a distribution of second-order quadrupolar interaction, which is characteristic of a poorly organized structure. The isotropic chemical shifts of the two resonances have been estimated by simulation at about 60 and 180 ppm that are characteristic of gallium in sixfold (Ga_{VI}) and fourfold (Ga_{IV}) coordination to oxygen, respectively (Figure S2). Characteristic NMR parameters are given in Table S1. The spectra are very similar to that of Ga in solid solution in alumina or $(Ga,Al)_2O_3$ mixed oxides.[26,29] Consequently, it can be inferred that gallium is inserted in a large part in the Al_2O_3 framework. The relative abundance of Ga_{IV} sites increases from 65 % for Ga/Al_{d_N2} to 80 % Ga/Al, which could be related to $(Ga,Al)_2O_3$ with Ga:Al between 1:3 and 1:6. These Ga_{IV} sites are reported to be the active sites for PDH presenting weak LAS.[29] For 15 wt.% Ga/Al_2O_3, Bardool and co-workers[30] also obtained ^{71}Ga MAS NMR spectrum typical of Ga in solid solution, and the presence of the solid solution was confirmed by extended X-ray absorption fine structure (EXAFS). X-ray absorption near edge structure (XANES) showed similar spectra for 15 wt.% and lower Ga contents (3, 6, 9, 12 wt.%) corresponding to Ga^{3+} tetracoordinated,[30] and the high dispersion of Ga, in the form of isolated ions even at high content (15 wt.%), with no formation of Ga clusters, was confirmed.

^{27}Al MAS NMR spectra of the three samples are composed of two main resonances attributed to tetracoordinated Al, Al_{IV} (δ_{iso} = 74 ppm) and Al in octahedral position, Al_{VI} (δ_{iso} = 15 ppm). Additional, pentacoordinated Al_V sites are observed in the case of Ga/Al_d. All the estimated NMR parameters are given on Table S2. Isotropic chemical shift, and quadrupolar coupling constant are quasi equivalent, which indicate no modification of aluminium environment. This result is coherent with XRD analyses indicating that the γ-Al_2O_3 structure is not modify. The very small difference in Al IV, V an VI population can be related to the incorporation of gallium in the surface of alumina.

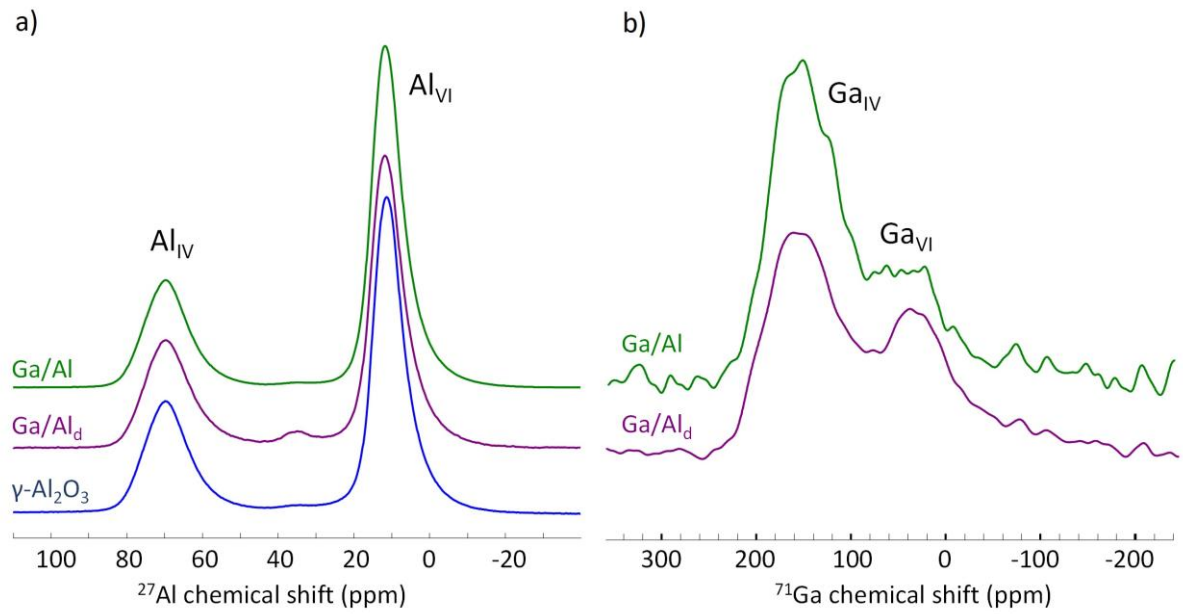

Figure 2. a) ^{27}Al and b) ^{71}Ga MAS NMR spectra, acquired respectively at $\nu 0$ (^{27}Al) = 221.6 MHz /νrot = 30 kHz and $\nu 0$ (^{71}Ga) = 259.3 MHz /νrot = 60 kHz for Ga/Al, Ga/Al_d pretreated under N_2 at 575°C, and for γ-Al_2O_3 (as reference).

The good dispersion of Ga species was confirmed by TEM and SEM for the Ga/Al and Ga/Al_d catalysts, where no Ga nanoparticle was seen, while the presence of Ga at the surface of the catalyst was confirmed *via* EDX and EDS (Figure S3, Figure S4), with a Ga surface content, determined at various locations on the samples, ranged from 5.4-5.9 wt.% for Ga/Al and 5.1-6.0 wt.% for Ga/Al_d samples.

In order to follow the decomposition of the gallium precursor salt in the various conditions used in the present study, *i.e.*, during calcination, during heating under inert atmosphere and during reduction, TGA-DTG analysis was performed on the Ga/Al_d catalyst heated under air, nitrogen and hydrogen. Results presented in Figure S5 show similar profiles whatever the gas composition. There are two main phenomena, one between 100 and 300 °C and a second one around 400 °C. It was demonstrated on unsupported gallium nitrate precursor that the decomposition and dehydration of gallium nitrate under air yield N_2O_5 and $Ga(OH)_2(NO_3)$ around 100 °C; these latter are decomposed into $Ga(OH)_3$ and N_2O_5 between 136 and 150 °C, and finally the hydroxide species are dehydrated to Ga_2O_3 at 460 °C.[31] Consequently, it can be inferred from the results of Figure S5 that whatever the type of treatment, oxidizing, decomposing or reducing, the nitrate species of the precursor salt are removed before 300 °C, and no modification of the catalyst occurs after 450 °C.

The effect of a thermal treatment under H_2 on the catalysts was studied by H_2-TPR and the results for γ-Ga_2O_3, Ga/Al and Ga/Al_d are presented in Figure 3. Before TPR, the calcined sample Ga/Al was pretreated under air at 350 °C and the uncalcined one Ga/Al_d under N_2 at 450 °C (see details in Supporting information). It should be noted that during the TPR, temperature was let at 650 °C during 1 h, temperature of reducing pretreatment before catalytic test, before heating up to 1000 °C. As shown in Figure 3 (a), the prepared gallium oxide sample presents two peaks of hydrogen consumption, at 350 °C and 650 °C, the latter being the smaller one. It has been reported in the literature that pure gallium oxide does not exhibit reduction peaks at temperatures below 600 °C if it is present under the α- or β- phases, contrary to the γ- phase, which displays a reduction peak at 350 °C, as in the present case, associated to the reduction at the surface by oxygen abstraction in Ga_2O_3, due to the high dispersion and low crystallinity of the γ-Ga_2O_3 polymorph.[32] On the other hand, Jochum and co-workers studied in depth the H_2 uptake on β-Ga_2O_3 combining temperature-programmed reduction and desorption experiments and concluded that hydrogen can interact with this gallium oxide from 30 °C, the interaction process evolving further according to the temperature: (i) from 30 °C until 200 °C, H_2 is weakly adsorbed *via* a homolytic way on available terminal oxygen species, (ii) at 200 °C, Ga-H species begin to be formed resulting from a heterolytic H_2 adsorption, (iii) above 280 °C, the formation of oxygen vacancies occurs from water abstraction, leading to the surface reduction and then to a stronger homolytic H_2 adsorption preferentially at the newly formed cus-Ga sites.[33] This same behavior was evidenced by Collins and co-workers to occur on the three polymorphs α-, β-, and γ- Ga_2O_3.[34] The reduction of pure Ga_2O_3 to metallic gallium is only possible at high temperature under ultra-high vacuum conditions and is explained by the disproportionation of Ga^+ cations according

to the reaction: 3 $Ga^{+} \rightarrow 2\ Ga^{0} + Ga^{3+}$.[35] In the present case, the reduction to Ga^{+} is more probable, since no reduction peak is seen after 650 °C. Considering the theoretical H_2 consumption needed to fully reduce Ga^{3+} into Ga^{+} (10.7 mmol H_2 g_{Ga2O3}^{-1}), the proportion of Ga^{3+} species that could be reduced around 350 °C was close to 0.4 %, in the same range as the value reported in the literature (< 2 %),[32] with a total reduction of 0.44 % after 650 °C (Table S3). Results displayed in Figure 3 (b, c) show that gallium species in Ga/Al and Ga/Al_d catalysts present in common three peaks of H_2 consumption around 400, 650 and 900 °C, the consumption peak at the highest temperature being the most significant in terms of peak area. On 5 wt. % Ga/Al_2O_3 catalysts prepared by impregnation followed by a calcination step at 550-600 °C, Xu and co-workers identified no reduction peaks below 600 °C during TPR analysis,[36] whereas Shao *et al.* identified a first reduction peak from 450 °C until 750 °C followed by a second one at 900°C attributed to Ga_2O_3 species with different dispersion states.[37] Based on the results of the literature obtained with Ga_2O_3 supported on zeolite, they attributed the first reduction peak to well-dispersed gallium species in the alumina and the peak at 900°C to the reduction of bulk Ga_2O_3. As in the present study the peaks around 400 °C and 650 °C are similar to those observed on the γ-Ga_2O_3 sample, we propose that the same gallium oxide species are probably present on the alumina support, corresponding to small crystallites of Ga_2O_3.[37] By contrast, the additional reduction peak, around 900 °C, could be due to the gallium species in strong interaction with the support, possibly inserted in the alumina framework, favored by the good dispersion of gallium species, leading to their reduction at higher temperatures. Values of hydrogen consumption at the various reduction peaks reported in Table S3 show that the amount of Ga^{3+} species reduced into Ga^{+} that could be obtained at the reduction temperature of 650 °C, temperature used for the reducing pretreatment before the propane dehydrogenation reaction, is approximately 3 % and 7 % for the Ga/Al and Ga/Al_d, respectively (considering the theoretical H_2 consumption needed to fully reduce Ga^{3+} into Ga^{+} equal to 702 µmol H_2 g_{cat}^{-1}). A total of 15 % and 22 % of reduction, respectively, is reached for each sample when the reduction is performed at temperatures over 900 °C (Table S3). According to Sun and co-workers,[23] H_2 treatment at 600 °C of Ga_2O_3/Al_2O_3 catalyst, where Ga_2O_3 is present in the form of nanoparticles at the alumina surface, allows reducing close to 25 % of the surface Ga species to $Ga^{\delta+}$. In the present study, a higher reduction temperature is needed to reach such a reduction level, in line with the good dispersion of the gallium species evidenced by electron microscopy on the calcined and uncalcined samples (Figures S3 and S4) and suggested by XRD and NMR results. It was checked by TEM and SEM that, after reduction at 650 °C (1 h), there were no significant changes in the surface of the catalyst and in the dispersion of Ga species (Figures S6 and S7). The Ga surface content, determined by EDS at various locations on the samples, ranged from 5.7 to 5.9 wt.% for Ga/Al_{red} and from 5.1 to 5.5 wt.% for the Ga/Al_{d_red} sample.

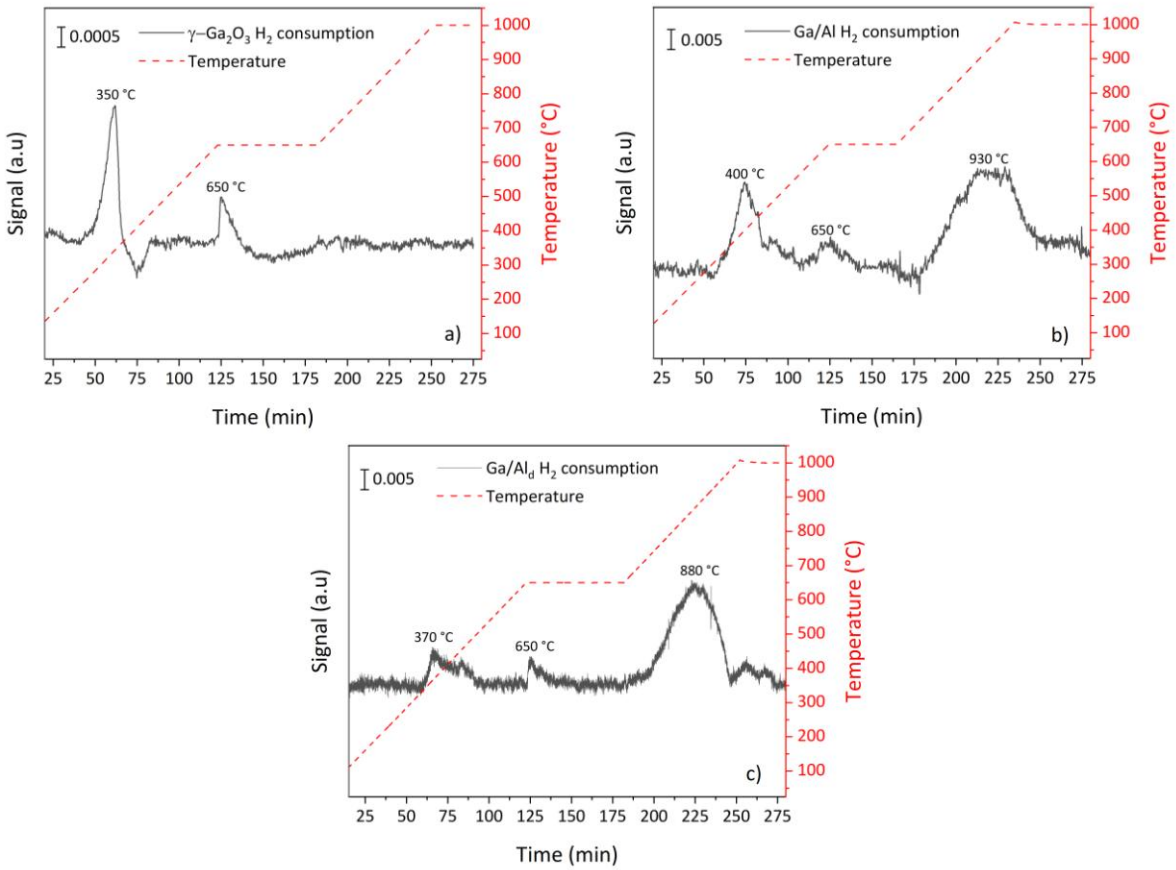

Figure 3. TPR profiles in function of time and temperature for a) γ-Ga_2O_3, b) Ga/Al, and c) Ga/Al_d catalysts in flow of 10 % H_2/Ar until 1000 °C.

Ga_2O_3, Ga/Al and Ga/Al_d samples were characterized by X-ray photoelectron spectroscopy (XPS) in order to check the oxidation state of the various catalysts before and after treatment under H_2 at 650°C (Results not shown). Only a +III oxidation state was observed, irrespective of the pretreatment, with no shift in the peak after reduction compared to the non-reduced sample (Bond energy of Ga3d : 20.4 ± 0.2 eV). This result can be attributed to the low hydrogen consumption of these samples during TPR. Even considering that the hydrogen consumption corresponds to the reduction of Ga^{3+} into Ga^{+}, the contribution to the XPS signal of the Ga species with oxidation state inferior to +III will be minimal.

It is reported in the literature that the activity of Ga-based catalyst in propane dehydrogenation depends on Lewis acid sites, while Brønsted acid sites are responsible for secondary reactions.[38] FTIR experiments of pyridine desorption according to temperature (Py-FTIR) were carried out to determine the type, amount, and strength of acid sites at the catalyst surface. Figure 4 shows FTIR profiles for the support and catalysts pretreated under vacuum at 575 °C, or under H_2 at 650 °C and subsequently under vacuum, (i) in the *ν*(OH) region (3600 – 3800 cm^{-1}) before the pyridine adsorption (Figure 4 (a)), and (ii) in the pyridine vibration region after its adsorption and desorption at 150 °C (Figure 4 (b)).

After treatment under vacuum, the spectrum of Al_2O_3 on Figure 4 (a) is typical of transitional gamma alumina, with representative bands at 3790, 3775, 3730 and 3682 cm^{-1} attributed to the stretching of OH groups coordinated to Al ions,[39,40] species with some acid character except for the last band at 3682 cm^{-1}. For the unsupported γ-Ga_2O_3, only a small band at 3692 cm^{-1} is visible, showing that after pretreatment under vacuum at 575 °C, the surface of this oxide is only slightly hydroxylated, possibly presenting Ga^{3+}-OH groups. In the case of the calcined catalyst (Ga/Al), minor modifications compared to bare alumina are observed. On the contrary, when no calcination is performed (Ga/Al_d), a significant decrease in all the representative alumina bands is observed. It can be inferred that gallium species probably resulting from thermal decomposition of the metal precursor after pretreatment at 575 °C under vacuum are very well dispersed at the alumina surface.

More information about the acidity of the materials is obtained in the 1650 – 1400 cm^{-1} region where the bands of adsorbed pyridine can be seen after adsorption followed by a thermodesorption at 150 °C (Figure 4 (b)). The γ-Al_2O_3 support exhibited four characteristic IR absorption peaks at 1620 cm^{-1} (ν_{8a}), 1576 cm^{-1}, 1494 cm^{-1} (ν_{19a}), and 1451 cm^{-1} (ν_{19b}), which could be attributed to the interaction of pyridine species with LAS.[39,41] No band is observed at 1640 or 1545 cm^{-1}, which correspond to pyridinium ions formed on Brønsted acid sites (BAS). This absence suggests that, even if BAS are present, they lack sufficient strength to protonate pyridine.[17,24,39] There is no change in the number of bands and band position when gallium is deposited on the alumina support for both the calcined and uncalcined samples. The unsupported γ-Ga_2O_3 sample displays a Py-FTIR profile similar to that of γ-Al_2O_3, with only a slight shift of ν_{8a} vibration band towards lower wavenumber. This is in accordance with the results obtained by Vimont and co-workers.[42] The Lewis acid sites of the γ-Ga_2O_3 sample are assigned to cus-Ga^{3+} at the oxide surface. From ν_{19b} vibration band, it is possible to quantify the amount of LAS. For the unreduced samples, the concentration of LAS given per gram of catalyst in Table 2 decreases in the following order: Ga/Al > γ-Al_2O_3 > Ga/Al_d > Ga_2O_3, being the Ga/Al sample that presents the highest acidity. The same ranking is obtained if the concentration is expressed per surface unit. Consequently, the gallium oxide species produced by calcination and dispersed on alumina (Ga/Al) are likely to be more acidic than the alumina support. When gallium precursor is impregnated on alumina and not calcined (Ga/Al_d), the gallium species decrease the acidity of the support, so they are probably less acidic than their calcined counterpart. Finally, even if the concentration of LAS is different, all the catalysts present roughly the same LAS distribution, with around 50 % of weak acid sites and around 25 % of medium and of strong acid sites as observed on the lone alumina support the alumina support.

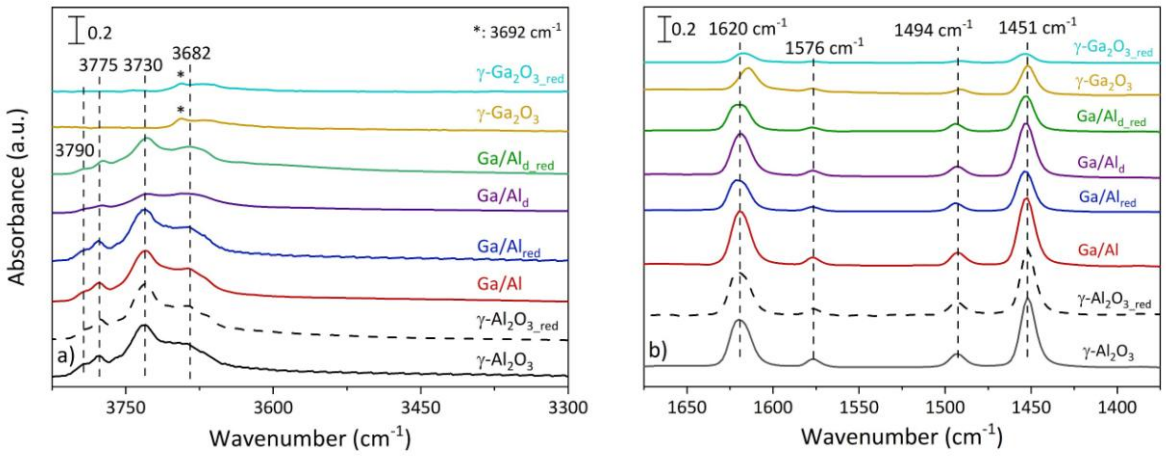

Figure 4. FTIR spectra of support and catalysts after pretreatment under vacuum at 575 °C (γ-Al_2O_3, γ-Ga_2O_3, Ga/Al and Ga/Al_d) or after reduction pretreatment under H_2 at 650 °C for 1 h and subsequently vacuum (γ-$Al_2O_{3\_red}$, γ-$Ga_2O_{3\_red}$, Ga/Al_{red} and Ga/Al_{d_red}): (a) in the OH stretching region, and (b) in the region of pyridine vibration after its adsorption and thermodesorption at 150 °C.

When the catalysts are pretreated under H_2 at 650 °C and subsequently treated under vacuum, the FTIR spectra in the ν(OH) region are slightly modified, except for the Ga/Al_d sample (Figure 4 (a)). Thus, for this uncalcined catalyst, broad bands in the 3800 – 3650 cm^{-1} region, similar to those observed on alumina, are more visible after reduction, suggesting that the dispersion of the gallium species decreased after the reducing pretreatment. An important decrease in LAS concentration is observed for Ga/Al_{red} and Ga/Al_{d_red} catalysts, of the same order of magnitude equal to 35 – 40 % compared to the unreduced counterparts (Table 2). It should be mentioned that the alumina support alone presents only a slight decrease in the acidity of approximately 7 %. Consequently, the decrease in the acidity of the Ga/Al and Ga/Al_d samples after reduction is mainly due to the decrease in the acidity brought by the gallium oxide species. This is confirmed by the fact that the impact of the reduction on the acidity of the unsupported gallia is very important, with only 34 % of the acidity of the sample maintained after reduction. Finally, while on pure γ-Ga_2O_3 the H_2 pretreatment leads to an increase in the proportion of weak LAS, it does not modify the LAS distribution for Ga/Al and Ga/Al_d samples, probably because the alumina support contributes also to the acidity. Castro-Fernández and co-workers[14] observed that the H_2 treatment leads to an increase of the fraction of strong LAS in γ-Ga_2O_3 and to an increase of the fraction of weak LAS in β-Ga_2O_3. Thus, the increase of the fraction of weak LAS in the Ga_2O_3 sample observed in the present study, could be attributed to a transition from the γ-phase to the β-phase. To check this point, XRD analyses was performed on

the reduced samples (Figure S8) showing similar XRD patterns for the reduced and non-reduced samples. Only for the unsupported Ga_2O_3 sample, the peaks are slightly better defined suggesting a better crystallisation of this sample after reduction. One can note that the decrease in the surface area after the reducing pretreatement (Table S4 compared to Table 1) is negligible compared to the calcined Ga_2O_3 sample (104 *vs* 122 m^2 g^{-1}). As no peak attributable to β-Ga_2O_3 are seen on the pattern of the reduced Ga_2O_3 sample, it can be inferred that, if the transition to the β-phase occurs during reduction, it is likely to be limited at the surface of the γ-Ga_2O_3 sample. The preservation of a BET surface area greater than 100 m^2 g^{-1} after reductive treatment also confirms that, since the β-Ga_2O_3 phase has a much smaller BET surface area.[34]

Table 2. Lewis acid sites (LAS) concentration and distribution in different catalysts and support determined by Py-FTIR after pretreatment under vacuum at 575 °C (γ-Al_2O_3, Ga/Al, Ga/Al_d, γ-Ga_2O_3) or under H_2 at 650 °C then vacuum (γ-$Al_2O_{3\_red}$, Ga/Al_{red}, Ga/Al_{d_red}, γ-$Ga_2O_{3\_red}$).

Sample	LAS concentration (µmol g^{-1})	LAS distribution		
		Weak sites (%)	Medium sites (%)	Strong sites (%)
γ-Al_2O_3	334	48	25	27
γ-$Al_2O_{3\_red}$	309	44	26	30
Ga/Al	357	49	23	28
Ga/Al_{red}	211	50	21	29
Ga/Al_d	286	50	28	22
Ga/Al_{d_red}	188	55	19	26
γ-Ga_2O_3	140	47	30	23
γ-$Ga_2O_{3\_red}$	48	61	22	17

PDH test in the absence of reductive pretreatment and H_2 co-feeding

The reaction conditions used in this study, different from those normally reported in the literature, especially the high $C_3H_8/(N_2 + H_2)$ ratio and WHSV values, were chosen in order to obtain lower conversion and favor the deactivation process. The absence of external mass transfer limitations was checked by varying the flow rate and the mass of catalysts while maintaining a constant WHSV (59 h^{-1}).[43] The catalysts and support, pretreated under N_2, were evaluated for propane dehydrogenation in the absence of H_2; results are shown in Figure 5. Values of conversion, activity, yields in the various products, propylene selectivity in gas phase, carbon balance and carbon deposited on the samples obtained at the beginning and at the end of the test (after 4 h time-on-stream (TOS)) are reported in Table 3.

Table 3. Performance of various materials for propane dehydrogenation (Pretreatment conditions: T = 575 °C, N_2, 60 mL min^{-1}; Reaction conditions: T = 575 °C, WHSV = 59 h^{-1}, $C_3H_8/N_2/H_2$ = 50/50/0, total flowrate = 100 mL min^{-1}, mass of catalyst = 100 mg).

Sample	X (%)[a]	k_d (h^{-1})	a_{C3H8} (mol h^{-1} g_{Ga}^{-1})[a]	a_{C3H8} (mol h^{-1} g_{cat}^{-1})[a]	Y (%)[a]					S_{C3H6} in gas phase (%)[a]	C balance (%)[a,b]	C deposited (wt.%)[c]
					CH_4	C_2H_6	C_2H_4	C_3H_6	$+C_4$			
γ-Ga_2O_3	7.4 (1.6)	0.39	0.13 (0.03)	0.10 (0.02)	< 0.1 (0.0)	0.0 (0.0)	< 0.1 (< 0.1)	5.2 (0.9)	0.0 (0.0)	98.9 (98.9)	97.8 (99.3)	n.d.
γ-Al_2O_3	1.8 (1.4)	0.06	n.d (n.d)	0.02 (0.02)	< 0.1 (< 0.1)	0.0 (0.0)	0.1 (0.1)	0.3 (1.1)	0.0 (0.0)	73.6 (88.3)	98.7 (99.9)	n.d.
Ga/Al	19.6 (12.8)	0.13	5.42 (3.54)	0.26 (0.17)	0.1 (< 0.1)	< 0.1 (0.0)	0.1 (0.1)	7.5 (2.6)	0.3 (0.0)	93.9 (95.3)	88.4 (89.9)	3.9

Ga/Al_d	20.7 (13.6)	0.13	5.73 (3.76)	0.28 (0.18)	< 0.1 (< 0.1)	< 0.1 (< 0.1)	0.1 (< 0.1)	10.4 (4.2)	0.0 (0.0)	98.5 (98.6)	89.8 (90.6)	2.7

[a] Values at initial, 1 min, and final, 4 h, TOS, outside and inside brackets, respectively; [b] Mass of carbon species at the outlet divided by the mass of carbon species at the inlet. [c] Determined by CHNS analysis on the spent samples after 4 h TOS. n.d.: No data available.

The alumina support was used to verify that it is not active, showing low propane conversion, which could be ascribed to the catalytic capability of cus Al^{3+} to dissociate H-H and C-H bonds,[24] with an initial selectivity of propene of *ca.* 74 % in gas phase. Similarly, a PDH test was carried out on the γ-Ga_2O_3 sample, showing an initial conversion of 7.4 %, yielding c.a. 98.9 % of propene selectivity in gas phase similar to the Ga/Al_d catalyst (98.5 %). This high selectivity for propene is associated with the low conversion of propane, which is related to the high WHSV chosen in the present study and the fact that propene is a primary product of PDH.[30] This material exhibited a rapid deactivation with a deactivation rate constant of 0.39 h^{-1}, compared to 0.13 h^{-1} for the Ga/Al and Ga/Al_d catalysts, with a final conversion of 1.6 %, similar to that obtained on bare γ-Al_2O_3. It should be noted that on a γ-Ga_2O_3 sample with the same BET surface area, Zheng and co-workers obtained a higher initial propane conversion (21 %) at 500 °C but in more favorable conditions, with highly diluted propane (2 % in N_2), a very low flowrate, and a much lower WHSV value.[44]

In the case of Ga-supported catalysts, a reference test was carried out by mixing physically the γ-Ga_2O_3 oxide with the γ-Al_2O_3 support for obtaining a 5.0 wt.% Ga reference catalyst; the profile was quite similar to the one of the bare alumina (Results not shown). The calcined and uncalcined samples showed no significant difference in the initial conversion and profile, presenting an initial conversion of around 20 % which decreases to around 13 % after 240 min of reaction regardless the treatment after catalyst synthesis; the deactivation on these materials occurs mainly at the beginning of the reaction (Figure 5 (a)). It should be noted that, for both catalysts, the initial carbon balance is low, slightly lower than 90 %. However, the amount of carbon deposited obtained by CHNS analysis on the calcined sample (3.9 wt.%) is higher compared with the uncalcined sample (2.7 wt.%), which is in accordance with its higher acidity (Table 2). The amount of carbon deposited was also analyzed by TPO, obtaining similar results. The presence of two kinds of coke can be evidenced by TPO on spent catalysts, soft coke oxidized generally at temperatures as low as 150 – 200 °C, and hard coke with increased degree of graphitization at temperature near 400 °C.[45] TPO on the spent calcined and uncalcined catalysts exhibited a single peak of coke oxidation to CO and CO_2 after 400 °C, the hard coke being then in bigger proportion (Figure S9 (a,b)).

Despite both Ga/Al_2O_3 samples exhibit similar conversion, a difference in the propene selectivity in gas phase is observed, being close to 94 % for the Ga/Al catalyst, while superior to 98 % for the Ga/Al_d one. This difference could also be attributed to the acidity exhibited by both catalysts, the Ga/Al sample presenting the highest LAS concentration, along with the highest proportion of strong LAS (28 %) in comparison with the Ga/Al_d (22 %), thus leading to the formation of methane and $+C_4$ by-products, not observed with Ga/Al_d (Table 3). More importantly, the proportion of Brønsted acid sites, evaluated by the activity of the catalysts for an isomerization reaction, responsible for by-products formation, is twice less for Ga/Al_d sample than for Ga/Al, the highest level of Brønsted acid sites being observed on the bare alumina support (Table S5).

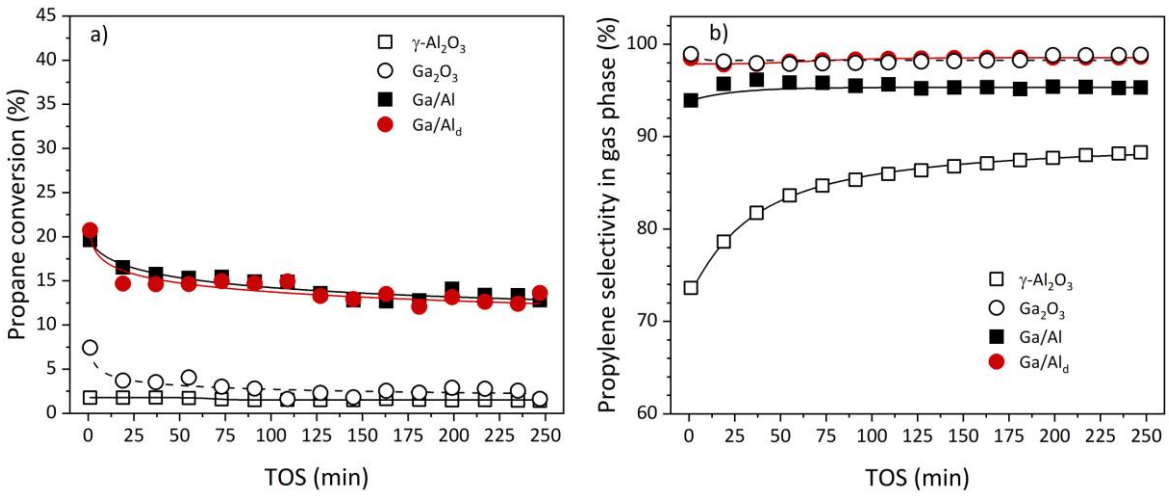

Figure 5. (a) Propane conversion and (b) propylene selectivity in gas phase as a function of time-on-stream (TOS) for various samples: γ-Al_2O_3, γ-Ga_2O_3, Ga/Al, Ga/Al_d. (Pretreatment conditions: T = 575 °C, N_2, 60 mL min^{-1}; Reaction conditions: T = 575 °C, WHSV = 59 h^{-1}, $C_3H_8/N_2/H_2$ = 50/50/0, total flowrate = 100 mL min^{-1}, mass of catalyst = 100 mg).

Effect of H_2 co-feeding during the PDH test performed in the absence of reductive pretreatment

To understand the role of hydrogen co-feeding in the propane dehydrogenation reaction, tests with 0 and 50 % H_2 in the feed gas were carried out with the Ga/Al catalyst unreduced before PDH. Considering only the reaction of propane dehydrogenation into propylene and H_2, the propane conversion, calculated at the thermodynamic equilibrium at 575 °C, will be 49.3 % and 25 % in the reaction conditions chosen, for a $C_3H_8/N_2/H_2$ gas mixture of 50/50/0 and 50/0/50, respectively. Consequently, from a thermodynamic point of view, the addition of H_2 in the gas stream has a negative effect on the conversion of propane to propene. As shown by the experimental results presented in Figure 6 (a) and detailed in Table 4, the initial propane conversion slightly varied, from 19.6 to 17.6 %, according to the hydrogen concentration, the highest conversion being obtained without H_2 co-feeding, in accordance with the thermodynamics. The initial and final propane conversions decrease in the same order: 0 % H_2 > 50 % H_2. Further to the H_2 co-feeding, an improvement in the carbon balance was observed (approximately 5 % increase of the global balance at the beginning of the reaction). In line with this result, a significant reduction of carbon deposited is observed with 50 % H_2 co-feeding compared to the test performed without H_2 (0.9 wt.% *vs* 3.9 wt.%). Then, it can be inferred that large hydrogen flows during PDH help to keep the catalyst surface clean of coke. However, the initial selectivity of propylene in gas phase remained around 94 %, regardless the H_2 amount in the feed. The propylene selectivity increases slightly with time-on-stream for 50 % of H_2 in the stream (Figure 6 (b)). Surprisingly, when large amount of H_2 is present in gas phase, methane production is virtually suppressed and ethylene production decreases with time-on-stream, while they are the two major by-products in the absence of H_2 co-feeding after 250 min TOS (Figure S10). Consequently, it can be supposed that the presence of large amount of H_2 in gas phase has an effect, not only on the reaction mechanisms, but also on the nature of the active sites present during the reaction.

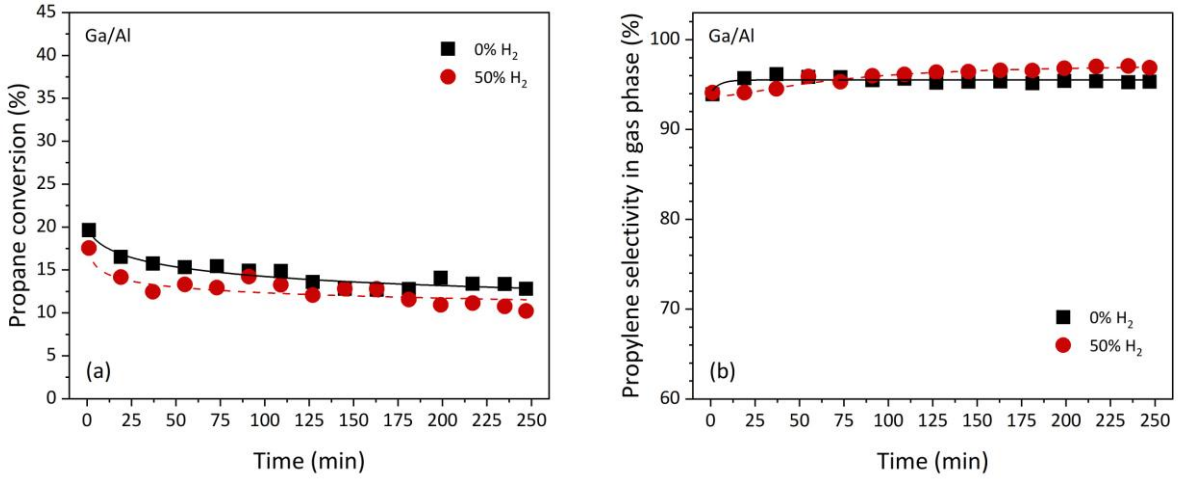

Figure 6. Effect of H_2 co-feeding on PDH performance over Ga/Al as a function of time-on-stream. (a) Propane conversion and (b) propylene selectivity in gas phase. (■) $C_3H_8/N_2/H_2$ = 50/50/0, (●) $C_3H_8/N_2/H_2$ = 50/0/50. (Pretreatment conditions: T = 575 °C, N_2, 60 mL min^{-1}. Reaction conditions: T = 575 °C, WHSV = 59 h^{-1}, total flowrate = 100 mL min^{-1}, mass of catalyst = 100 mg).

These results are not in line with those obtained by Zhou and co-workers,[24] who observed an increase in propane conversion with the increase of H_2 in the gas stream up to 10 %, without any effect on the deactivation rate, while the production of propene in gas phase was stable versus time-on-stream in the presence of H_2 co-feeding. This divergent behavior could be due to the strong difference in the reaction conditions. Zhou and co-workers used a very small propane flowrate, lower WHSV value and varied the C_3H_8/H_2 molar ratio between 0.5 (C_3H_8/H_2 = 10/20) and 2 (C_3H_8/H_2 = 10/5).[24] In these conditions, more H_2 is introduced in the flow, combined with a higher contact time, which may be beneficial to the reduction of the catalyst, in addition to the dilution of the propane feed by nitrogen performed systematically by these authors. In the present study we used harsher conditions, with high WHSV value and a C_3H_8/H_2 molar ratio of 1 (C_3H_8/H_2 = 50/50). Consequently, to better understand the effect of the H_2 co-feeding, it seems important to start the reaction with a pre-reduced catalyst in order to better control the surface state of the catalyst.

Table 4. Performance of calcined Ga/Al catalyst for propane dehydrogenation at different H_2 co-feedings (Pretreatment conditions: T = 575 °C, N_2, 60 mL min^{-1}; Reaction conditions: T = 575 °C, WHSV = 59 h^{-1}, total flowrate = 100 mL min^{-1}, mass of catalyst = 100 mg).

Gas mixture ($C_3H_8/N_2/H_2$)	X (%)[a]	k_d (h^{-1})	a_{C3H8} (mol h^{-1} g_{Ga}^{-1})[a]	a_{C3H8} (mol h^{-1} g_{cat}^{-1})[a]	Y (%)[a]					S_{C3H6} in gas phase (%)[a]	C balance (%)[a,b]	C deposited (wt.%)[c]
					CH_4	C_2H_6	C_2H_4	C_3H_6	$+C_4$			
50/50/0	19.6 (12.8)	0.13	5.42 (3.54)	0.26 (0.17)	0.1 (< 0.1)	< 0.1 (0.0)	0.1 (0.1)	7.5 (2.6)	0.3 (0.0)	93.9 (95.3)	88.4 (89.9)	3.9
50/0/50	17.6 (10.2)	0.16	4.85 (2.82)	0.24 (0.14)	< 0.1 (< 0.1)	0.2 (< 0.1)	0.2 (0.1)	9.8 (6.9)	0.1 (< 0.1)	94.1 (96.9)	92.9 (96.9)	0.9

[a] Values at initial,1 min, and final, 4 h, TOS, outside and inside brackets, respectively; [b] Mass of carbon species at the outlet divided by the mass of carbon species at the inlet. [c] Determined by CHNS analysis on the spent samples after 4 h TOS.

Effect of H_2 pretreatment without H_2 co-feeding during the PDH test

The effect of reduction temperature on the performance of propane dehydrogenation was evaluated by imposing a reductive pretreatment of the Ga/Al catalyst at the reaction temperature (575 °C) and at 650 °C, temperature necessary to ensure the reduction of a small part of the Ga species in the catalyst according to TPR results (Table S3). Compared to the catalyst pretreated under N_2, the reductive treatment induced a lower initial conversion, leading to an initial propane conversion of around 17 % with a deactivation rate of about 0.30 h^{-1} and no significant change in the carbon balance, regardless the reduction temperature (Table 5). Therefore, H_2 pretreatment decreases the number of active species. A redistribution of gallium species over the alumina support during the reductive treatment is unlikely given the absence of change of the FTIR spectra in the hydroxyl region after H_2 pretreatment of this sample (Figure 4 (a)). Finally, the selectivity towards propylene was improved by reducing the Ga/Al catalyst, the reduced sample presenting a selectivity higher than 98 % after 25 min of reaction until the end (Figure 7), which could be explained by the decrease of Brønsted acid sites responsible for by-products formation (Table S5). In the following, the reducing pretreatment will be performed at 650 °C.

Table 5. Performance of Ga/Al catalyst for propane dehydrogenation at different pretreatment conditions (Reaction conditions: T = 575 °C, WHSV = 59 h^{-1}, $C_3H_8/N_2/H_2$ = 50/50/0, total flowrate = 100 mL min^{-1}, mass of catalyst = 100 mg).

Pretreatment	X (%)[a]	k_d (h^{-1})	a_{C3H8} (mol h^{-1} g_{Ga}^{-1})[a]	a_{C3H8} (mol h^{-1} g_{cat}^{-1})[a]	Y (%)[a]					S_{C3H6} in gas phase (%)[a]	C balance (%)[a,b]
					CH_4	C_2H_6	C_2H_4	C_3H_6	$+C_4$		
N_2 – 575 °C	19.6 (12.8)	0.13	5.42 (3.54)	0.26 (0.17)	0.1 (< 0.1)	< 0.1 (0.0)	0.1 (0.1)	7.5 (2.6)	0.3 (0.0)	93.9 (95.3)	88.4 (89.9)
H_2 – 575 °C	17.2 (5.9)	0.30	4.72 (1.61)	0.23 (0.08)	< 0.1 (< 0.1)	< 0.1 (0.0)	0.3 (< 0.1)	6.6 (2.2)	0.0 (0.0)	94.8 (98.2)	89.8 (96.4)
H_2 – 650 °C	17.1 (5.8)	0.30	4.72 (1.60)	0.23 (0.08)	< 0.1 (< 0.1)	0.0 (0.0)	0.2 (< 0.1)	5.2 (2.2)	< 0.1 (0.0)	96.2 (98.9)	88.3 (96.5)

[a] Values at initial, 1 min, and final, 4 h, TOS, outside and inside brackets, respectively; [b] Mass of carbon species at the outlet divided by the mass of carbon species at the inlet.

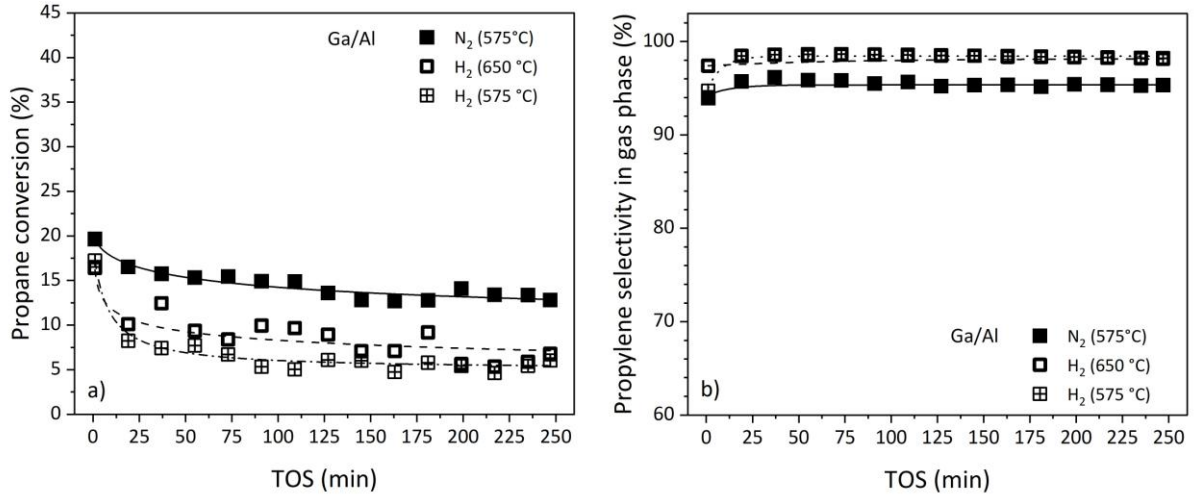

Figure 7. Evolution of (a) propane conversion, and (b) propylene selectivity in gas phase as a function of time-on-stream during PDH test with different pretreatment conditions over Ga/Al catalyst: (■) calcination, T = 575 °C under N_2, (□) reduction at T = 650 °C under H_2 for 1 h, (⊞) reduction at T = 575 °C under H_2 for 1 h. (Reaction conditions: T = 575 °C, WHSV = 59 h^{-1}, $C_3H_8/N_2/H_2$ = 50/50/0, total flowrate = 100 mL min^{-1}, mass of catalyst = 100 mg).

Effect of H_2 pretreatment with H_2 co-feeding during the PDH test

Based on the experimental results obtained with H_2 co-feeding, it appears that the presence of H_2 in gas phase during PDH reaction modifies the catalytic performance of the Ga/Al catalyst in a negative way when this sample is used without any reductive pretreatment (Table 4). Thus, the effect of hydrogen co-feeding on the performance of Ga/Al_{red} and Ga/Al_{d_red} catalysts was studied after reduction under H_2 and further catalytic test at 575 °C with 50 % propane in the presence of a small amount of H_2 (5 %, balanced in N_2), of a larger one (50% H_2), and without H_2 in the feed for comparison. Results are presented in Figure 8 and summarized in Table 6.

First of all, it can be seen that in the absence of H_2 co-feeding, Ga/Al_{d_red} presents lower initial and final conversions than its non-reduced counterpart, as it was previously observed for Ga/Al_{red}, with an initial conversion of 11.8 % after reduction instead of 20.7 % when it is unreduced, *i.e.,* a decrease by a factor of 43 %. This higher fall of activity after reduction for the Ga/Al_{d_red} catalyst compared to Ga/Al_{red} may be explained by the higher reducibility of gallium species leading to less active sites, since the decrease in the concentration of LAS was similar in both catalysts. Also, the decrease in surface area, from 194 to 107 m^2 g^{-1}, may have a negative effect on the activity (Tables 1 and S4). It can be noted that an increase in the amount of carbon deposited from 2.7 for the unreduced catalyst to 5 wt.% for the Ga/Al_{d_red} sample is also observed. Concerning the deactivation, it is more pronounced for both reduced catalysts than for the non-reduced Ga/Al and Ga/Al_d samples, with a deactivation rate constant around 0.32 h^{-1} compared with 0.13 h^{-1} respectively. The pre-reduction has a beneficial effect on the formation of propene for the Ga/Al sample, for which the initial selectivity of propene in gas phase increases from 93.9% for the non-reduced catalyst to 96.2 % once the catalyst is pretreated under H_2. which may be related to the decrease in weak Brønsted acid sites observed after reduction of this catalyst (Table S5). Finally, pretreatment under H_2 of the γ-Ga_2O_3 sample showed no significant change in propane conversion, compared with the calcined sample pretreated under N_2, and a slight decrease in the formation of propylene (Figure S11).

Table 6. Performance of Ga/Al_{red} and Ga/Al_{d_red} catalysts on propane dehydrogenation at different H_2 co-feedings after H_2 pretreatment at 650 °C for 1 h (Reaction conditions: T = 575 °C, WHSV = 59 h^{-1}, total flowrate = 100 mL min^{-1}, mass of catalyst = 100 mg).

Gas mixture ($C_3H_8/N_2/H_2$)	X (%)[a]	k_d (h^{-1})	a_{C3H8} (mol h^{-1} g_{Ga}^{-1})[a]	a_{C3H8} (mol h^{-1} g_{cat}^{-1})[a]	Y (%)[a]					S_{C3H6} in gas phase (%)[a]	C balance (%)[a,b]	C deposited (wt.%)[c]
					CH_4	C_2H_6	C_2H_4	C_3H_6	$+C_4$			
Ga/Al_{red}												

50/50/0	17.1 (5.8)	0.30	4.72 (1.60)	0.23 (0.08)	< 0.1 (< 0.1)	0.0 (0.0)	0.2 (< 0.1)	5.2 (2.2)	< 0.1 (0.0)	96.2 (98.9)	88.3 (96.5)	2.0
50/45/5	16.3 (8.8)	0.18	4.50 (2.43)	0.22 (0.12)	< 0.1 (< 0.1)	< 0.1 (0.0)	0.2 (< 0.1)	6.1 (3.3)	0.0 (0.0)	96.3 (96.7)	90.0 (94.5)	4.0
50/0/50	17.8 (13.2)	0.09	4.91 (3.64)	0.24 (0.18)	< 0.1 (< 0.1)	0.2 (< 0.1)	0.3 (0.1)	7.0 (4.8)	0.2 (< 0.1)	90.7 (96.5)	89.9 (91.8)	0.8
Ga/Al_{d_red}												
50/50/0	11.8 (3.3)	0.34	3.30 (0.92)	0.16 (0.04)	< 0.1 (< 0.1)	< 0.1 (0.0)	0.1 (< 0.1)	6.2 (2.2)	0.0 (0.0)	97.3 (97.9)	94.5 (98.9)	5.0
50/45/5	16.8 (8.4)	0.20	4.67 (2.35)	0.22 (0.11)	< 0.1 (< 0.1)	< 0.1 (0.0)	0.2 (< 0.1)	10.1 (3.2)	0.0 (0.0)	97.3 (98.5)	93.6 (94.9)	4.2
50/0/50	10.5 (8.1)	0.07	2.93 (2.26)	0.14 (0.11)	< 0.1 (< 0.1)	0.1 (< 0.1)	0.1 (0.1)	5.4 (4.4)	0.0 (0.0)	96.5 (97.5)	95.1 (96.4)	2.1

[a] Values at initial, 1 min, and final, 4 h, TOS, outside and inside brackets, respectively; [b] Mass of carbon species at the outlet divided by the mass of carbon species at the inlet. [c] Determined by CHNS analysis on the spent samples after 4 h TOS.

As shown in Figure 8, for Ga/Al_{red}, the initial propane conversion is not affected by the presence of H_2 co-feeding, contrary to what was observed with the unreduced sample (Figure 6 (a)). For the Ga/Al_{d_red} sample, a positive effect of H_2 co-feeding on the initial conversion is only observed with 5 % of H_2 in the gas stream, with an increase in conversion from 11.8 % (0 % H_2) to 16.8 % (5 % H_2). The major effect of H_2 co-feeding in the pre-reduced materials is seen in the deactivation, with final conversions higher than in the absence of H_2 in the gas stream regardless the catalyst. Moreover, the k_d deactivation constant decreases as the amount of H_2 in the stream increases. In addition, the initial selectivity of propene in gas phase is in the 96 – 98% range whatever the catalyst and the amount of H_2 in the stream, except for 50 % H_2 and Ga/Al_{red} catalyst for which this percentage is initially around 90 %, mainly due to a higher production of ethane, ethylene and $+C_4$ compounds during reaction (Figure S12), while the formation of by-products is strongly limited on Ga/Al_{d_red} (Figure S13). On the other hand, it can be noted that, in general, the Ga/Al_{red} sample exhibits higher activity and lower carbon deposition compared to the Ga/Al_{d_red}. As for the non-reduced samples, the increase of H_2 co-feeding favours the decrease of carbon species deposited on the catalyst surface, since the carbon deposit is the lowest with 50 % H_2 co-feeding for both catalysts. In conclusion of all these observations, it can be inferred that the Ga species and their distribution on the alumina support vary according to the nature of their original state before reduction, *i.e.,* gallium oxide or just impregnated gallium nitrate, which is in line with the characterization results, especially the acidity of the catalyst and the hydrogen consumption during TPR.

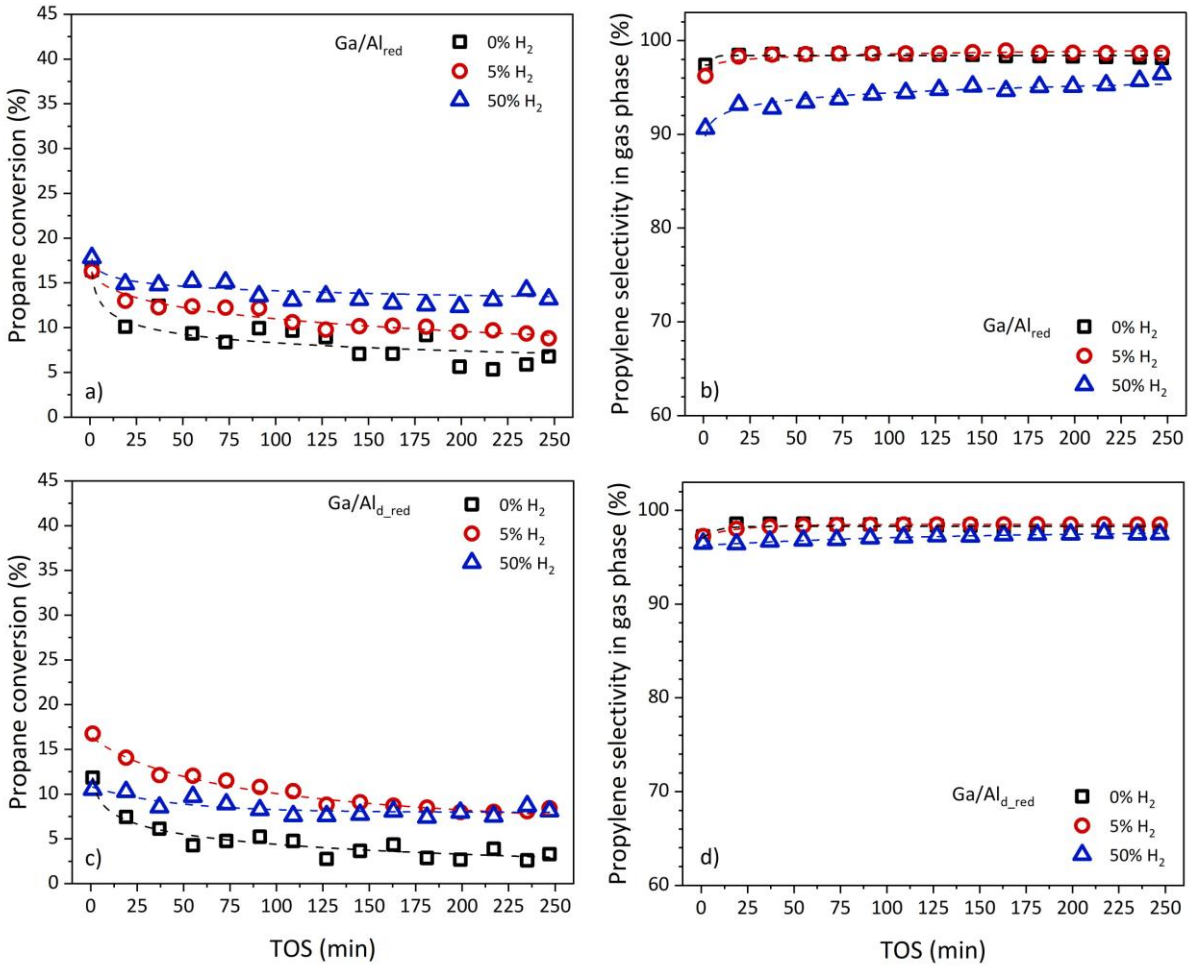

Figure 8. Effect of H_2 co-feeding on PDH performance as a function of time-on-stream of (a, b) Ga/Al$_{red}$ and (c, d) Ga/Al$_{d_red}$ catalysts after reduction pretreatment at 650 °C for 1 h: (□) $C_3H_8/N_2/H_2$ = 50/50/0, (○) $C_3H_8/N_2/H_2$ = 50/45/5, (Δ) $C_3H_8/N_2/H_2$= 50/0/50. (Reaction conditions: T = 575 °C, WHSV = 59 h^{-1}, total flowrate: 100 mL min^{-1}, mass of catalyst: 100 mg).

To further elucidate the role of H_2 in the course of the PDH reaction and obtain more information about the surface sites capable of dissociating this molecule, FTIR spectra were collected for γ-Al_2O_3 support, γ-Ga_2O_3, Ga/Al, and Ga/Al$_d$ catalysts after reduction pretreatment under H_2 flowing. Figure 9 shows FTIR profiles obtained for all samples after hydrogen pretreatment at 650 °C, recorded either under flowing H_2 (60 mL min^{-1}) or under vacuum. It is observed that two main regions in the spectra (in grey in Figure 9) appeared for the calcined and uncalcined samples, Ga/Al and Ga/Al$_d$, once hydrogen was introduced in the cell: a band associated to the Ga-H vibrations (2050 – 1900 cm^{-1}) accompanied by a broad band between 3600 and 3450 cm^{-1} ascribed to the stretching vibration of the OH groups, not present on the non-reduced samples, that could be ascribed to -OH near the Ga^{3+} centers.[24] Clearly, the appearance at the same time of the bands corresponding on the one hand to hydrides and to the other hand to hydroxyl groups shows that, on our catalysts, the H_2 dissociation on Ga^{3+}-O is heterolytic giving rise to Ga^{3+}H-OH. For the alumina support, no peak in the hydride region was observed regardless the treatment, while the γ-Ga_2O_3 sample exhibited an intense peak in the Ga-H region and no peak in the 3600 – 3450 cm^{-1} range, the bands of hydroxyls appearing at higher wavenumber, between 3700 and 3600 cm^{-1}, in the typical range observed for Ga_2O_3.[42] It should be noted that the present results for the supported catalysts are very different from those reported in the literature[23,24] , which indicated during the reduction process the disappearance on Ga_2O_3/Al_2O_3 catalysts of the bands around 3540 cm^{-1}, attributed to Ga-OH species, due to the removal of O atoms through dehydroxylation, while the ones linked to Ga-H species appear and increase as a function of time. It should be noted that in the paper of Sun and co-workers,[23] Ga_2O_3 nanoparticles with diameters around 4 nm, were clearly identified. Then, it can be inferred that the bands in the OH region observed in the present study on the supported gallium catalysts for which Ga species are in strong interaction with the support, and probably inserted in the alumina framework in surface, could be due to the presence of Ga^{3+}-O-Al^{3+} sites where the heterolytic

dissociation of H_2 leads to $Ga^{3+}H\text{-}OH\text{-}Al^{3+}$, the strong interaction with alumina making it difficult to lose the oxygen atom through dehydroxylation. After reduction treatment and under H_2 flowing, the two peaks at ca. 2020 and 1980 cm^{-1} corresponding to the Ga-H band are more intense in the Ga/Al_{d_red} sample (Table S6). According to the literature, the high and low frequency Ga-H bands at ca. 2020 and 1980 cm^{-1} correspond to Ga_{IV}-H and Ga_{VI}-H sites,[34] which are formed by heterolytic dissociation of H_2 molecule over Ga-O bonds yielding gallium hydrides and hydroxyl species.[22] It can be seen that for both Ga/Al_{red} and Ga/Al_{d_red} samples, Ga_{VI}-H is predominant on the surface, whereas NMR analysis indicated that the more active Ga_{IV} is dominant on the non-reduced samples. Therefore, the lower activity of the reduced catalysts compared to the non-reduced ones could be attributed to the increased presence in surface of less active Ga_{VI} sites after reduction. Furthermore, the evolution of the GaH_x species while increasing the reduction temperature was investigated (Figure S14). For both catalysts (Ga/Al and Ga/Al_d), no peak related with GaH_x species was observed at low temperatures. However, the intensity of the Ga-H band increased upon reaching 575 °C, and a more pronounced peak was observed at the maximum reduction temperature (650 °C). One can note that after reduction at 575°C and 650 °C, the amount of GaH_x species is much lower on Ga/Al_{red} than on Ga/Al_{d_red} (Table S7). Given the small proportion of GaH_x species determined by FTIR on the Ga/Al_{red} sample at 575 °C under pure H_2 flowing, it must be inferred that during the reaction of propane dehydrogenation under 5 % H_2 in the flow, and even under 50 % H_2, the amount of gallium hydrides species is negligible on the catalysts surface. Consequently, the improvement of the catalytic properties, particularly in terms of limiting deactivation, observed after H_2 pretreatment and with H_2 co-feeding can hardly be attributed to the only presence of GaH_x species. Probably, the decrease in the number of Lewis acid sites induced by the presence of H_2 may play a role, allowing a good balance between GaH_x species and Ga^{3+} or $Ga^{\delta+}$ species. Finally, the gallium hydride and hydroxyl signals disappeared when the sample was no longer exposed to H_2 flow and subsequently purged under N_2, inducing H_2 desorption by the recombination of hydrogen (Figure S15).

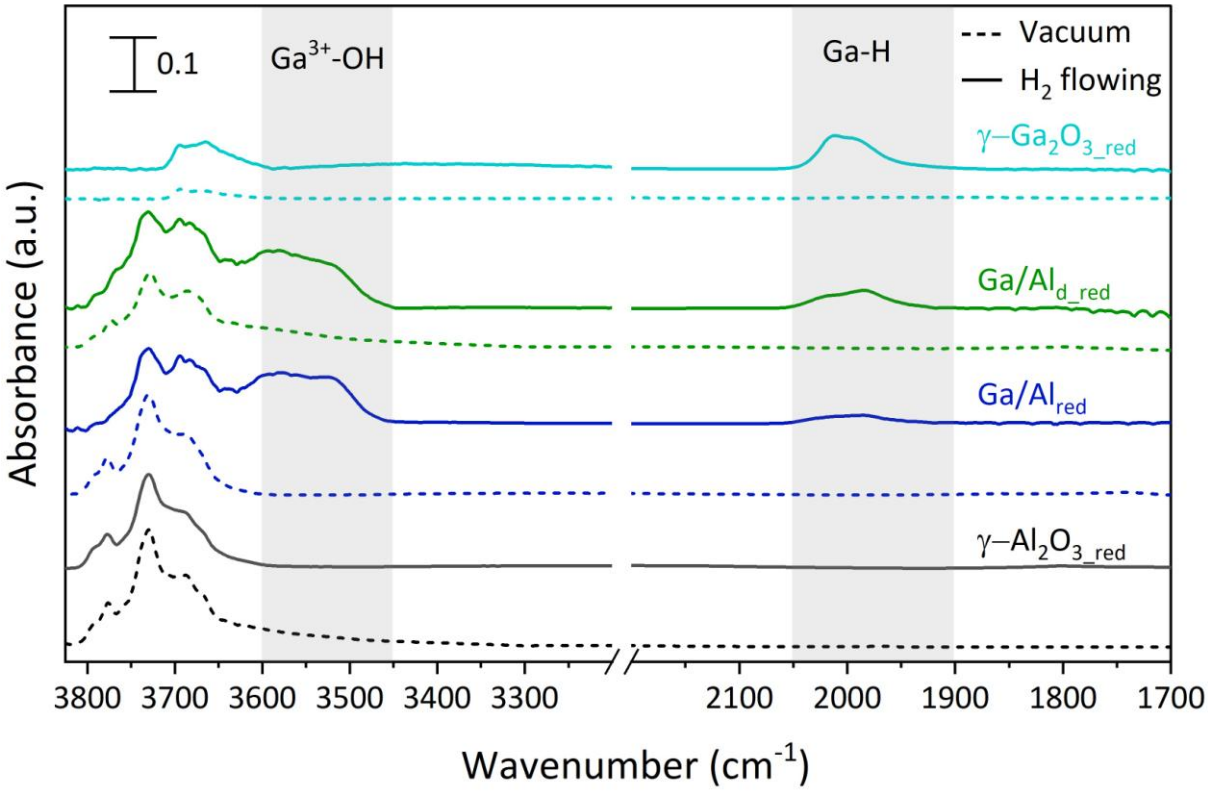

Figure 9. FTIR spectra of support and catalysts in the Ga-OH and Ga-H stretching regions after pretreatment under H_2 at 650 °C, recorded after H_2 flow stop and vacuum (dashed lines) or under H_2 flow (solid lines).

Finally, as it was demonstrated that the presence of 50 %H_2 as co-feed limits the deactivation of the catalysts, long-term stability tests were performed on Ga/Al_{red} and Ga/Al_{d_red} samples. Results, shown in Figure 10, confirm the high stability of the catalysts, especially for the Ga/Al_{d_red} one, in the presence of large amounts of H_2 in the feed, compared to the same test performed without H_2. In addition, for both catalyst, propylene selectivity consistently maintained above 95%

when large amount of H_2 is co-fed, while the propylene selectivity decreases in function of the time when no H_2 it is co-fed.

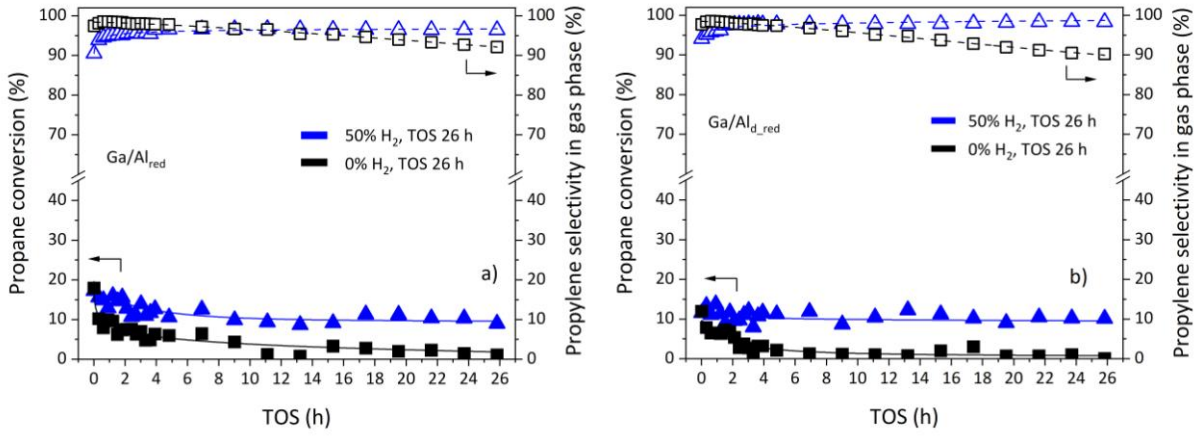

Figure 10. Long term stability test on a) Ga/Al$_{red}$ and b) Ga/Al$_{d_red}$ catalysts after reduction pretreatment at 650 °C for 1 h: (□) $C_3H_8/N_2/H_2$ = 50/50/0, (Δ) $C_3H_8/N_2/H_2$= 50/0/50. (Reaction conditions: T = 575 °C, WHSV = 59 h^{-1}, total flowrate: 100 mL min^{-1}, mass of catalyst: 100 mg, TOS: 26 h)

Conclusion

This work was devoted to the study of a 5 wt.% Ga/Al_2O_3 catalyst for PDH, obtained after impregnation of the nitrate precursor salt on the alumina support and drying (Ga/Al$_d$ sample) and then after calcination (Ga/Al sample). For both samples, XRD and TEM analyses revealed that the gallium species were probably well dispersed at the surface of the support, even inserted in the alumina framework according to NMR analysis. TPR experiments revealed that the reduction pretreatment performed at 650 °C (reduction temperature used before the PDH test) could reduce a few Ga^{3+} species in Ga^{+}, approximately 3 % and 9 % for the Ga/Al and Ga/Al$_d$, respectively. Thus, the strong interaction of gallium with alumina limits strongly its reduction. Consequently, the adsorption of H_2 on the reduced Ga/Al and Ga/Al$_d$ catalysts occurs by heterolytic dissociation. Under the studied reaction conditions, *i.e.*, under a high $C_3H_8/(N_2+ H_2)$ ratio, it was observed that H_2 co-feeding had a negative impact on propane conversion and selectivity of propylene in gas phase when the catalyst has not undergone a reductive pretreatment before PDH. On the other hand, it was observed that reduction pretreatment before the PDH reaction performed in the absence of hydrogen co-feeding reduced the activity, being this effect more significant in the Ga/Al$_d$ uncalcined catalyst. This decrease in activity was associated with a reduction in the amount of LAS clearly observed by Py-FTIR. However, reduction pretreatment of the catalysts improved the propylene selectivity in gas phase for the Ga/Al sample, which can be attributed to the decrease in the proportion of Brønsted acid sites responsible for the formation of by-products. Additionally, the major effect of H_2 co-feeding after reduction, regardless of the catalysts, was observed in the deactivation over time during PDH reaction. The deactivation rate constant (k_d) decreased as the amount of H_2 in the stream increased, linked to the constant recovery of active sites due to the removal of coke in the course of its formation, and the continuous formation of GaH_x sites on the surface of the catalyst as identified by FTIR analysis in the presence of hydrogen. Despite this, no direct relationship between the quantity of gallium hydrides species determined by FTIR on the catalysts and the catalytic performance in the propane dehydrogenation reaction was evidenced. The amounts of Lewis and Brønsted acid sites were demonstrated to be an important parameter for good catalytic performance in terms of activity and propylene selectivity.

Experimental

Catalyst preparation: Ga-based catalyst was prepared *via* wet impregnation. Briefly, γ-alumina, priori calcined at 600 °C, was put in contact with a $Ga(NO_3)_3.xH_2O$ solution at an initial pH of 3. The concentration of the gallium solution was adjusted in order to obtain catalyst with nominal Ga content of 5.0 wt.%. The slurry was shaken at room temperature and then the solvent was removed by rotary evaporator. After drying step, the supported catalyst was recovered and stored, or calcined for 4 h at 575 °C. The obtained catalysts were defined as Ga/Al and Ga/Al$_d$ for the catalyst with and without calcination step, respectively.

A non-supported gallia sample was prepared through an alcoholic precipitation pathway that demonstrated to lead to the gamma phase.[26,27] In a typical synthesis, $Ga(NO_3)_3.xH_2O$ was dissolved in ethanol. Then, concentrated aqueous ammonia (32 wt.%) and ethanol (50:50 in volume) were added dropwise under continuous stirring at room temperature until pH of 8.5 and no further precipitation occurred. The resulting alcogel was kept under stirring for 1 h, after which it was filtered, thoroughly washed with ethanol, dried overnight, and finally calcined at 575 °C for 4 h. The obtained non-supported sample was defined as γ-Ga_2O_3.

When the catalysts were *in-situ* reduced under H_2 flow after these preparation steps, the obtained materials were defined as Ga/Al_{red}, Ga/Al_{d_red} and γ-$Ga_2O_{3\_red}$. Ga/Al_d catalyst pretreated under N_2 at 575°C before some characterizations, was named Ga/Al_{d_red}.

Characterization: ICP-OES, nitrogen adsorption (BET method), XRD, TPR, TGA-DTG, TEM, SEM, solid-state NMR, XPS, CHNS analysis, TPO and FTIR spectroscopy were conducted to characterize the catalyst samples. The acidity of the catalysts was evaluated using pyridine adsorption and desorption followed by infrared spectroscopy (Py-FTIR), and the reaction of 3,3-dimethylbut-1-ene (33DMB1) isomerization.

PDH test: Propane dehydrogenation (PDH) reaction was carried out in a fixed-bed quartz reactor at atmospheric pressure. In a typical experiment, 100 mg of catalyst was loaded between two plugs of quartz wool and carborundum (SiC, 1.3 g, granulometry 210 µm). The catalyst was pretreated under N_2 flow at the reaction temperature of 575 °C. Then, the performance in propane dehydrogenation was evaluated at 575 °C by passing the reaction gas mixture through the reactor. The total flow rate was kept constant at 100 mL min^{-1}, the concentration of C_3H_8 was fixed at 50 % balanced in N_2 and the classical reaction time was 4 h (26 h for the long-term tests). The effect of H_2 co-feeding was evaluated in the same conditions. The reaction gas mixture consisted of 50 % propane mixed with 5 or 50 % H_2 balanced with N_2. The effect of a reductive pretreatment was studied by *in situ* pre-reduction of the catalyst under H_2 flow at 650 °C for 1 h. After reduction, the system was cooled down under H_2 to reaction temperature (575 °C) and the reaction gas mixture (containing or not H_2) was introduced at a flowrate of 100 mL min^{-1}. All the catalytic tests were carried out at a weight hourly space velocity (WHSV) of 59 h^{-1}, using an online Varian CP-3800 gas chromatograph equipped with a FID detector.

Supporting Information

Additional data and experimental details are given in the Supporting Information. Additional reference is also cited within the Supporting Information.[46–49]

Acknowledgements

The authors thank the CNRS for its financial support for collaboration between the INCAPE and IC2MP laboratories as part of the international research project OLECAT. The authors from IC2MP acknowledge financial support from the European Union (ERDF) and “Région Nouvelle Aquitaine” and indicate that this work pertains to the French government program "Investissements d'Avenir" (EUR INTREE, reference ANR-18-EURE-0010). The financial support from the IR INFRANALYTICS FR2054 for conducting the research is also gratefully acknowledged. The authors express their sincere gratitude to Christine Canaff for her contributions to the XPS analysis and to Julie Rosseau for her work on the TEM and SEM-EDS imaging.

Keywords: Propane dehydrogenation • Ga – based catalyst • H_2 co-feeding • Acidity • GaH_x sites

Reference

[1] S. Chen, X. Chang, G. Sun, T. Zhang, Y. Xu, Y. Wang, C. Pei, J. Gong, *Chem. Soc. Rev.* **2021**, *50*, 3315–3354.
[2] J. J. H. B. Sattler, J. Ruiz-Martinez, E. Santillan-Jimenez, B. M. Weckhuysen, *Chem. Rev.* **2014**, *114*, 10613–10653.
[3] T. K. Phung, T. L. M. Pham, K. B. Vu, G. Busca, *Journal of Environmental Chemical Engineering* **2021**, *9*, 105673.
[4] A. Akah, M. Al-Ghrami, *Applied Petrochemical Research* **2015**, *5*, 377–392.
[5] F. Feng, H. Zhang, S. Chu, Q. Zhang, C. Wang, G. Wang, F. Wang, L. Bing, D. Han, *Journal of Industrial and Engineering Chemistry* **2023**, *118*, 1–18.
[6] A. V. Lavrenov, L. F. Saifulina, E. A. Buluchevskii, E. N. Bogdanets, *Catalysis in Industry* **2015**, *7*, 175–187.
[7] Z.-P. Hu, D. Yang, Z. Wang, Z.-Y. Yuan, *Chinese Journal of Catalysis* **2019**, *40*, 1233–1254.
[8] B. Feng, Y.-C. Wei, W.-Y. Song, C.-M. Xu, *Petroleum Science* **2022**, *19*, 819–838.

[9] P. Castro-Fernández, D. Mance, C. Liu, I. B. Moroz, P. M. Abdala, E. A. Pidko, C. Copéret, A. Fedorov, C. R. Müller, *ACS Catal.* **2021**, *11*, 907–924.
[10] Y. Gu, H. Liu, M. Yang, Z. Ma, L. Zhao, W. Xing, P. Wu, X. Liu, S. Mintova, P. Bai, Z. Yan, *Applied Catalysis B: Environmental* **2020**, *274*, 119089.
[11] T. Otroshchenko, S. Sokolov, M. Stoyanova, V. A. Kondratenko, U. Rodemerck, D. Linke, E. V. Kondratenko, *Angewandte Chemie International Edition* **2015**, *54*, 15880–15883.
[12] D. Zhao, X. Tian, D. E. Doronkin, S. Han, V. A. Kondratenko, J.-D. Grunwaldt, A. Perechodjuk, T. H. Vuong, J. Rabeah, R. Eckelt, U. Rodemerck, D. Linke, G. Jiang, H. Jiao, E. V. Kondratenko, *Nature* **2021**, *599*, 234–238.
[13] S. J. Pearton, J. Yang, I. Cary Patrick H., F. Ren, J. Kim, M. J. Tadjer, M. A. Mastro, *Applied Physics Reviews* **2018**, *5*, 011301.
[14] P. Castro-Fernández, D. Mance, C. Liu, P. M. Abdala, E. Willinger, A. A. Rossinelli, A. I. Serykh, E. A. Pidko, C. Copéret, A. Fedorov, C. R. Müller, *Journal of Catalysis* **2022**, *408*, 155–164.
[15] Y. Liu, G. Zhang, J. Wang, J. Zhu, X. Zhang, J. T. Miller, C. Song, X. Guo, *Chinese Journal of Catalysis* **2021**, *42*, 2225–2233.
[16] H. Xiao, J. Zhang, P. Wang, X. Wang, F. Pang, Z. Zhang, Y. Tan, *Catal. Sci. Technol.* **2016**, *6*, 5183–5195.
[17] M. Chen, J. Xu, F.-Z. Su, Y.-M. Liu, Y. Cao, H.-Y. He, K.-N. Fan, *Journal of Catalysis* **2008**, *256*, 293–300.
[18] Y. Xu, X. Wang, D. Yang, Z. Tang, M. Cao, H. Hu, L. Wu, L. Liu, J. McLeod, H. Lin, Y. Li, Y. Lifshitz, T.-K. Sham, Q. Zhang, *ACS Catalysis* **2021**, *11*, 10159–10169.
[19] Y. Zhang, Y. Yu, R. Wang, Y. Dai, L. Bao, M. Li, Y. Zhang, Q. Liu, D. Xiong, Q. Wu, D. Shi, K. Chen, Y. Li, G. Jiang, E. V. Kondratenko, H. Li, *Journal of Catalysis* **2023**, *428*, 115208.
[20] C. S. Praveen, A. P. Borosy, C. Copéret, A. Comas-Vives, *Inorg. Chem.* **2021**, *60*, 6865–6874.
[21] P. Castro-Fernández, A. I. Serykh, A. V. Yakimov, I. P. Prosvirin, A. V. Bukhtiyarov, P. M. Abdala, C. Copéret, A. Fedorov, C. R. Müller, *Catalysis Science & Technology* **2022**, *12*, 3957–3968.
[22] I. Takahara, M. Saito, M. Inaba, K. Murata, *Catalysis Letters* **2004**, *96*, 29–32.
[23] G. Sun, Z.-J. Zhao, L. Li, C. Pei, X. Chang, S. Chen, T. Zhang, K. Tian, S. Sun, L. Zheng, J. Gong, *Nature Chemistry* **2024**, *16*, 575–583.
[24] S.-Z. Zhou, X.-Q. Gao, F. Wu, W.-C. Li, A.-H. Lu, *Applied Catalysis A: General* **2023**, *668*, 119488.
[25] F. Gashoul Daresibi, A. A. Khodadadi, Y. Mortazavi, *Applied Catalysis A: General* **2023**, *655*, 119117.
[26] C. O. Areán, M. R. Delgado, V. Montouillout, D. Massiot, *Zeitschrift für anorganische und allgemeine Chemie* **2005**, *631*, 2121–2126.
[27] M. Rodríguez Delgado, C. Otero Areán, *Materials Letters* **2003**, *57*, 2292–2297.
[28] K. Shimizu, A. Satsuma, T. Hattori, *Applied Catalysis B: Environmental* **1998**, *16*, 319–326.
[29] P. Castro-Fernández, M. Kaushik, Z. Wang, D. Mance, E. Kountoupi, E. Willinger, P. M. Abdala, C. Copéret, A. Lesage, A. Fedorov, C. R. Müller, *Chem. Sci.* **2021**, *12*, 15273–15283.
[30] R. Bardool, D. P. Dean, H. N. Pham, A. K. Datye, S. Raeissi, M. R. Rahimpour, J. T. Miller, *Journal of Catalysis* **2023**, *428*, 115201.
[31] V. Berbenni, C. Milanese, G. Bruni, A. Marini, *Journal of Thermal Analysis and Calorimetry* **2005**, *82*, 401–407.
[32] L. Li, W. Wei, M. Behrens, *Solid State Sciences* **2012**, *14*, 971–981.
[33] W. Jochum, S. Penner, K. Föttinger, R. Kramer, G. Rupprechter, B. Klötzer, *Journal of Catalysis* **2008**, *256*, 268–277.
[34] S. E. Collins, M. A. Baltanás, A. L. Bonivardi, *Langmuir* **2005**, *21*, 962–970.
[35] A. I. Serykh, M. D. Amiridis, *Surface Science* **2009**, *603*, 2037–2041.
[36] B. Xu, B. Zheng, W. Hua, Y. Yue, Z. Gao, *Journal of Catalysis* **2006**, *239*, 470–477.
[37] C.-T. Shao, W.-Z. Lang, X. Yan, Y.-J. Guo, *RSC Adv.* **2017**, *7*, 4710–4723.
[38] L. Ni, R. Khare, R. Bermejo-Deval, R. Zhao, L. Tao, Y. Liu, J. A. Lercher, *J. Am. Chem. Soc.* **2022**, *144*, 12347–12356.
[39] A. Van Assche, C. Especel, A. Le Valant, F. Epron, *Molecular Catalysis* **2022**, *517*, 112059.
[40] V. Sanchez Escribano, G. Garbarino, E. Finocchio, G. Busca, *Topics in Catalysis* **2017**, *60*, 1554–1564.
[41] M. A. Tedeeva, A. L. Kustov, P. V. Pribytkov, G. I. Kapustin, A. V. Leonov, O. P. Tkachenko, O. B. Tursunov, N. D. Evdokimenko, L. M. Kustov, *Fuel* **2022**, *313*, 122698.
[42] A. Vimont, J. C. Lavalley, A. Sahibed-Dine, C. Otero Areán, M. Rodríguez Delgado, M. Daturi, *J. Phys. Chem. B* **2005**, *109*, 9656–9664.
[43] A. Farjoo, F. Khorasheh, S. Niknaddaf, M. Soltani, *Scientia Iranica* **2011**, *18*, 458–464.
[44] B. Zheng, W. Hua, Y. Yue, Z. Gao, *Journal of Catalysis* **2005**, *232*, 143–151.
[45] M. Wolf, N. Raman, N. Taccardi, M. Haumann, P. Wasserscheid, *ChemCatChem* **2020**, *12*, 1085–1094.
[46] M. Guisnet, P. Ayrault, J. Datka, *Polish Journal of Chemistry* **1997**, *71*, 1455–1461.
[47] C. Kemball, H. F. Leach, B. Skundric, K. C. Taylor, *Journal of Catalysis* **1972**, *27*, 416–423.
[48] D. Martin, D. Duprez, *Journal of Molecular Catalysis A: Chemical* **1997**, *118*, 113–128.
[49] A. Siahvashi, D. Chesterfield, A. A. Adesina, *Ind. Eng. Chem. Res.* **2013**, *52*, 4017–4026.

Entry for the Table of Contents

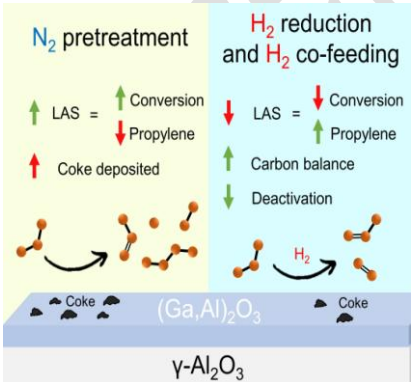

The effect of various pretreatment (N_2 or H_2) and feeding conditions were studied in the propane dehydrogenation over Ga_2O_3/Al_2O_3 catalysts. Changes in the speciation and the acidity (Lewis acid sites, LAS) of the catalyst were observed, confirmed by FTIR and TPR. The acidity was found to have a strong impact in the propane conversion and propylene selectivity.

Supporting Information

Ga_2O_3/Al_2O_3 CATALYSTS FOR PROPANE DEHYDROGENATION: EFFECT OF H_2 TREATMENT AND CO-FEEDING

Sebastian Amar Gil,*[a] Catherine Especel,[a] Francisco J. Passamonti,[b] Valérie Montouillout,[c] Viviana M. Benítez,*[b] Florence Epron*[a]

[a] S. Amar Gil, C. Especel, F. Epron
CNRS, Université de Poitiers, Institut de Chimie des Milieux et Matériaux de Poitiers-IC2MP, Poitiers, France
E-mail: florence.epron@univ-poitiers.fr, sebastian.amar.gil@univ-poitiers.fr

[b] F. J. Passamonti, V. M. Benítez
Instituto de Investigaciones en Catálisis y Petroquímica - INCAPE
Universidad Nacional del Litoral
Colectora Ruta Nac. Nº 168 Km. 0 - Paraje El Pozo, 3000 Santa Fe, Argentina
E-mail: vbenitez@fiq.unl.edu.ar

[c] V. Montouillout
Conditions Extrêmes et Matériaux: Haute Température et Irradiation, CEMHTI, UPR 3079 -CNRS Univ Orléans, Orléans, France

Experimental methods

Materials

γ-Alumina, with a surface area of 200 m^2 g^{-1}, was crushed and sieved to achieve a granulometry between 250 and 100 µm and used as support. Gallium nitrate hydrate ($Ga(NO_3)_3.xH_2O$, 99.9 % purity from Sigma-Aldrich), absolute ethanol (C_2H_6O, ≥ 99.9 % from Sigma-Aldrich) and ammonia (NH_3, 32 wt.% from VWR Chemicals) were used without further purification.

Characterization

Inductively coupled plasma optical emission spectroscopy (ICP-OES) was used for the determination of metal content of each sample. The measurements were performed with a Perkin Elmer Optima 2000DV spectrometer. The samples were previously digested in an acidic mixture of HNO_3 and HCl under microwave heating.

The textural properties of the catalysts were determined by N_2 adsorption at -196 °C (77 K) using a Micromeritics Tristar II PLUS. The specific surface area of the various catalysts was determined from the Brunauer-Emmet-Teller (BET) equation, the pore volume was determined by the Barrett-Joyner-Halenda (BJH) method, and the pore diameter was calculated as $4V_{total}/S_{BET}$.

Powder X-ray diffraction (XRD) patterns were recorded on a PANalytical EMPYREAN apparatus using Cu Kα radiation (λ_1 = 1.5406 Å) and an X'Celerator detector. Data were collected over a range of 10 ° to 90 ° with 0.1 ° steps and a dwell time of 900 s. Crystalline phases present in the samples were identified by comparison with standards of the ICSD database.

The temperature-programmed reduction (TPR) was measured in a programmable temperature system (Micromeritics Autochem 2920II apparatus). Prior to the analysis, the sample (0.2 g) was treated by dry argon at RT for 10 min, then the calcined samples (Ga_2O_3 and Ga/Al) were treated under air flow (30 mL min^{-1}) at 350 °C for 1 h, and the uncalcined sample (Ga/Al_d) under nitrogen flow (30 mL min^{-1}) at 450 °C for 1 h. Then the sample was let cool down under dry argon (30 mL min^{-1}). The system was fed with 10 % H_2/Ar (30 mL min^{-1}) and heated up from room temperature until 1000 °C with a heating rate of 10 °C min^{-1}, with a stop at 650 °C during 1 h. The consumption of H_2 was monitored by TCD.

Thermogravimetric (TGA) and differential thermogravimetric (DTG) analyses, using a Q600 TA Instrument apparatus, were performed to characterize the thermal decomposition of the catalysts under inert gas, dry air or hydrogen with a heating rate of 10 °C min^{-1} from room temperature to 900 °C.

Transmission electron microscopy (TEM) was performed with a JEOL 2100 UHR microscope equipped with an energy dispersive X-ray (EDX). The catalysts were ultrasonically dispersed in ethanol and the suspension was brought onto a copper grid with carbon film.
Scanning Electron Microscopy (SEM) was performed with a JOEL FEG 7900F electron microscope equipped with a Brücker Flat Quad detector (EDS). The catalysts were observed directly on powder and placed in the microscope chamber without metallization or other treatment. Chemical mapping and spotting were carried out using the Flat Quad detector.

The ^{27}Al and ^{71}Ga high resolution solid-state NMR spectra have been obtained on a Bruker NEO 850 spectrometer operating at 2XX MHz and 269 MH_Z respectively. ^{27}Al spectra have been acquired in 2.5 mm rotors spun at 30 kHz using a single pulse experiment ($\pi/18$, νRF= 100kHz). XX FID were accumulated with a recycling delay of 3s ensuring complete signal relaxation. The ^{71}Ga central transition has been acquired using rotor-synchronized whole-echo measurements and selective conditions of irradiation ($\pi/2$ pulse of 6 ms, νRF =50 kHz). 60 000 transients were accumulated with 1 s recycling delay.
The chemical shifts were referenced to $Al(NO_3)_3$ and $Ga(NO_3)_3$ 1 M solution. Quantification of the relative ratios, average isotropic chemical shift (δ_{iso}), distribution of isotropic chemical shift ($\Delta_i\delta_{so}$) and average quadrupolar coupling constant (C_Q) of the Al and Ga environments were estimated using the Gaussian isotropic model (GIM) or Czjzek model implemented in the DMFit software

Lewis acidity was evaluated using pyridine adsorption and desorption at 150, 250, 350, and 450 °C followed by Fourier transform infrared spectrometry in a Thermo Nicolet Nexus equipment (Py-FTIR). The sample was pressed in order to obtain a self-supported wafer with a diameter of 16 mm and introduced in an *in situ* cell and pretreated either at 575 °C under vacuum (10^{-6} bar) overnight or under H_2 at 650 °C for 1 h (from RT to 650 °C, 10 °C min^{-1}, 60 mL min^{-1}), and subsequently cooled down to 150 °C under vacuum. After achieving the pretreatment conditions, the background was registered on the empty cell. The wafer was exposed to pyridine vapor at 150 °C for 5 min and then evacuated for 1 h at 10^{-6} bar to collect the FTIR reference spectra. Then, the temperature was increased (5 °C min^{-1}) and the spectra were recorded at 250, 350, and 450 °C after evacuation for 1 h at each temperature. All the spectra, after subtraction of the background, were compared at a normalized sample weight of 30 mg. The amount of Lewis acid sites (LAS) was determined from the integrated area using the value of the molar extinction coefficient (1.28 cm µmol^{-1}) of the band at 1455 cm^{-1}.[46] The spectrum obtained at 150 °C was used to calculate the total amount of Lewis acid sites. The distribution of weak acid sites was calculated by difference between the surface area at 150 and 250 °C, the medium acid sites between 250 and 350 °C, while the amount of strong acid sites was directly determined from the spectrum at 350 °C.

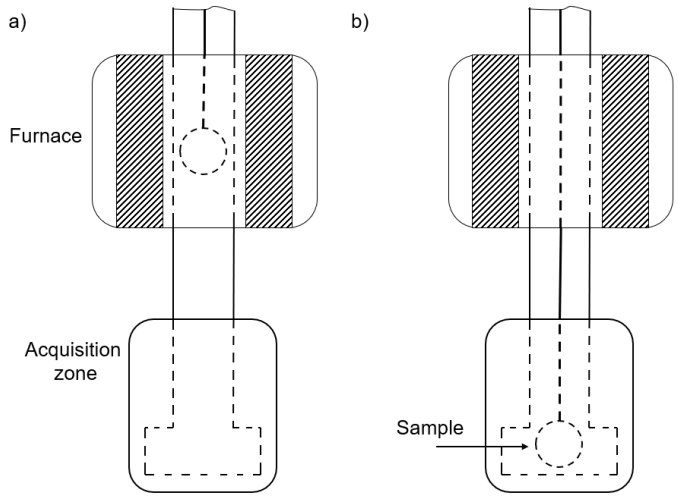

Example of IR setup while a) heating the self-supported waffle, and b) data acquisition.

$$LAS\ concentration = \frac{Area \times S}{\varepsilon \times m}$$

where $LAS\ concentration$, $Area$, S, ε and m represent the number of Lewis acid sites (in µmol g^{-1}), the integrated area (in cm^{-1}) of the band at 1455 cm^{-1}, the wafer surface (in cm^2), the extinction factor (in cm µmol^{-1}) and the sample weight (in g), respectively.

The FTIR spectra under hydrogen atmosphere were obtained using a Thermo Nicolet Nexus spectrometer, and the background was collected under hydrogen atmosphere after treating *in situ* the sample in a cell at 650 °C, for 1 h under H_2 flow (60 mL min^{-1}). Briefly, the catalyst was treated in a hydrogen atmosphere from room temperature to 650 °C, 10 °C min^{-1}, to resemble the reduction conditions used in the catalytic test. Once the reduction temperature was reached, infrared spectra were collected over time. Then, the system was purged under N_2 flow, and infrared spectra were collected.

The reaction of 3,3-dimethylbut-1-ene (33DMB1) isomerization was used to characterize the Brønsted acid sites, not enough strong on the studied catalysts to be probed by pyridine.[47,48] It is known that Lewis acid sites are not involved in this reaction. Catalyst samples (100 mg) were treated in flowing nitrogen (60 mL min^{-1}) at 575 °C, or in flowing hydrogen (60 mL min^{-1}) at 650 °C during 1 h and then cooled under nitrogen to the reaction temperature (250 °C). These pretreatment conditions were chosen in order to be similar to the ones used before propane dehydrogenation test. The isomerization reaction was carried out at 250 °C under a constant flow of 30 mL min^{-1} of N_2 saturated with 33DMB1. The reactants and the products were analyzed by on-line gas chromatography.

The amount of carbon deposited, after catalytic test, was determined by temperature programmed oxidation (TPO). The sample (25 mg) was heated up to 700 °C under air flow (40 mL min^{-1}) with a ramp of 10 °C min^{-1}. Exhaust gas was then treated in a methanizer reactor at 380 °C and the outlet gas was analyzed using a FID detector, and the total amount of carbon deposited was determined by comparing the area of the TPO traces with the area produced by reference 8 wt.% C sample. The amount of carbon deposited was also determined by combustion with a CHNS elemental analyzer (UNICUBE system).

PDH test

The outlet gas composition was analyzed by an online Varian CP-3800 gas chromatograph equipped with a FID detector, and a GS-Al/KCl capillary column.

The weight hourly space velocity (*WHSV*), propane conversion (*X*), activity (*a*), yield to each product C_xH_y (*Y*), carbon mass balance (*C*) and hydrocarbonselectivity in gas phase (*S*) were calculated as follows:

$$WHSV\ (h^{-1}) = \frac{F_{C_3H_{8in}} \times M_{C_3H_8}}{m}$$

$$X_{C_3H_8}(\%) = \frac{F_{C_3H_{8in}} - F_{C_3H_{8out}}}{F_{C_3H_{8in}}} \times 100$$

$$a_{C_3H_8}(mol\ h^{-1}\ g_{mt}^{-1}) = \frac{X \times F_{C_3H_{8in}}}{m \times \%_{mt}}$$

$$Y_{C_xH_y}(\%) = \frac{x \times F_{C_xH_y}}{3 \times F_{C_3H_8}} \times 100$$

$$C(\%) = \frac{C_{out}}{C_{in}} \times 100$$

$$S(\%) = \frac{x \times F_{C_xH_y}}{1 \times F_{CH_4} + 2 \times F_{C_2H_6} + 2 \times F_{C_2H_4} + 3 \times F_{C_3H_6} + 4 \times F_{C_4H_{10}} + 4 \times F_{C_4H_8}} \times 100$$

where $F_{C_3H_8}$ corresponds to the molar flowrate of propane (mol h^{-1}), and $F_{C_xH_y}$ refers to the molar flow rate of each product identified at the outlet (C_3H_6, C_2H_6, C_2H_4, CH_4, C_4H_{10} and C_4H_8); *in* and *out*, the molar flowrate at the inlet and at the outlet, respectively; x and y, the number of carbon and hydrogen atoms in the molecule, respectively; $M_{C_3H_8}$ the molar mass of propane (g mol^{-1}); m the mass of catalyst (g) and $\%_{mt}$ the percentage of metal in wt.% in the catalyst.

The catalyst stability was evaluated with a deactivation rate (k_d) estimated by first-order deactivation model:

$$k_d = \frac{\left\{Ln\left[\frac{1 - X_f}{X_f}\right] - Ln\left[\frac{1 - X_i}{X_i}\right]\right\}}{t}$$

where i and f stand for initial and final, and t for the PDH reaction time.

Reactions involved during propane dehydrogenation

During propane dehydrogenation, the following reactions may take place:[1,49]

$C_3H_8 \rightleftarrows C_3H_6 + H_2$ Equation (S1)

$C_3H_8 \rightleftarrows CH_4 + C_2H_4$ Equation (S2)

$C_3H_8 + H_2 \rightleftarrows C_2H_6 + CH_4$ Equation (S3)

$C_2H_4 + H_2 \rightleftarrows C_2H_6$ Equation (S4)

$C_3H_8 \rightleftarrows 3C + 4H_2$ Equation (S5)

Supporting Results

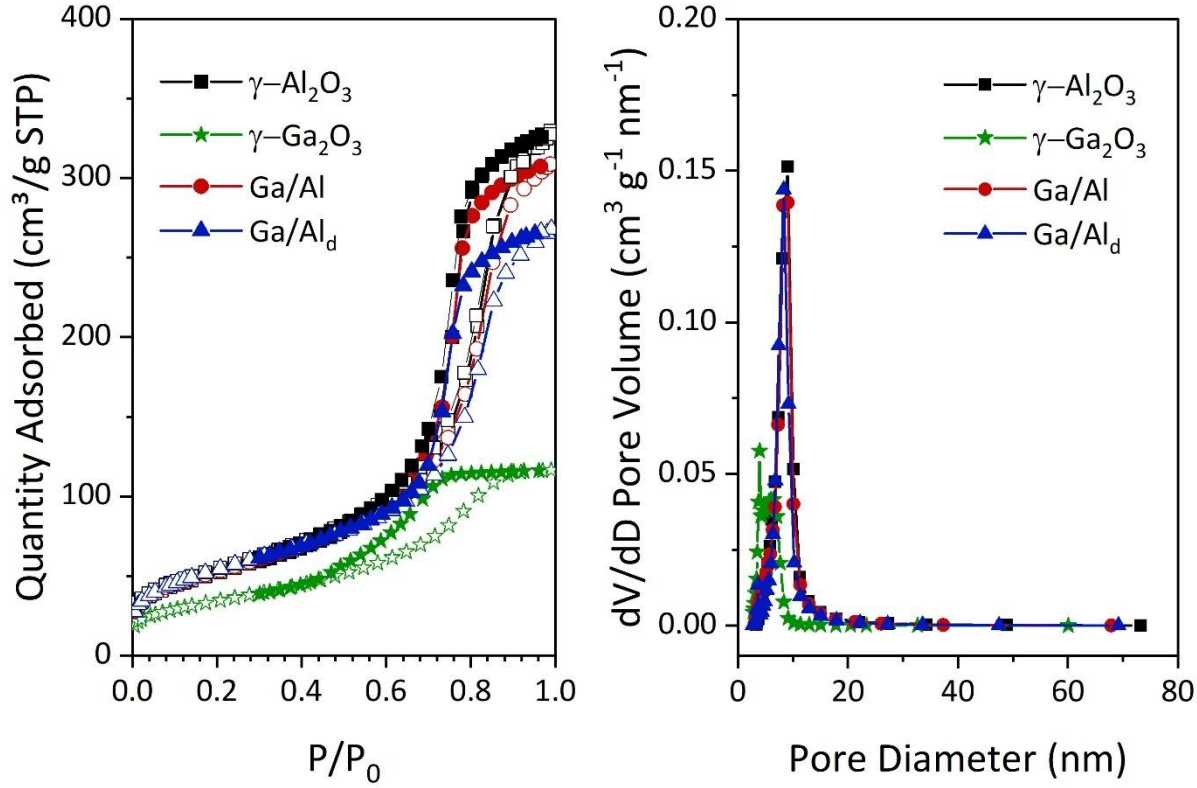

Figure S1. N_2 physisorption and pore size distribution of pure γ-Ga_2O_3, γ-Al_2O_3, Ga/Al, Ga/Al_d catalysts.

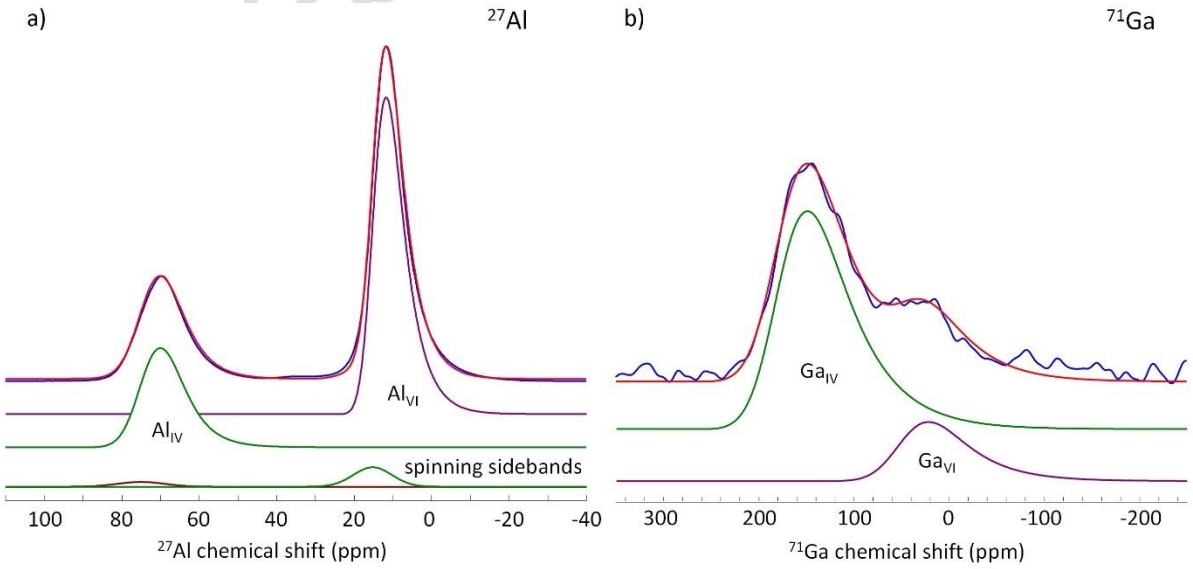

Figure S2. Experimental and calculated a) ^{27}Al and b) ^{71}Ga MAS NMR spectra of Ga/Al sample, acquired respectively at $\nu 0$ (^{27}Al) = 221.6 MHz /νrot = 30,kHz and $\nu 0$ (^{71}Ga) = 259.3 MHz /νrot = 60 kHz.

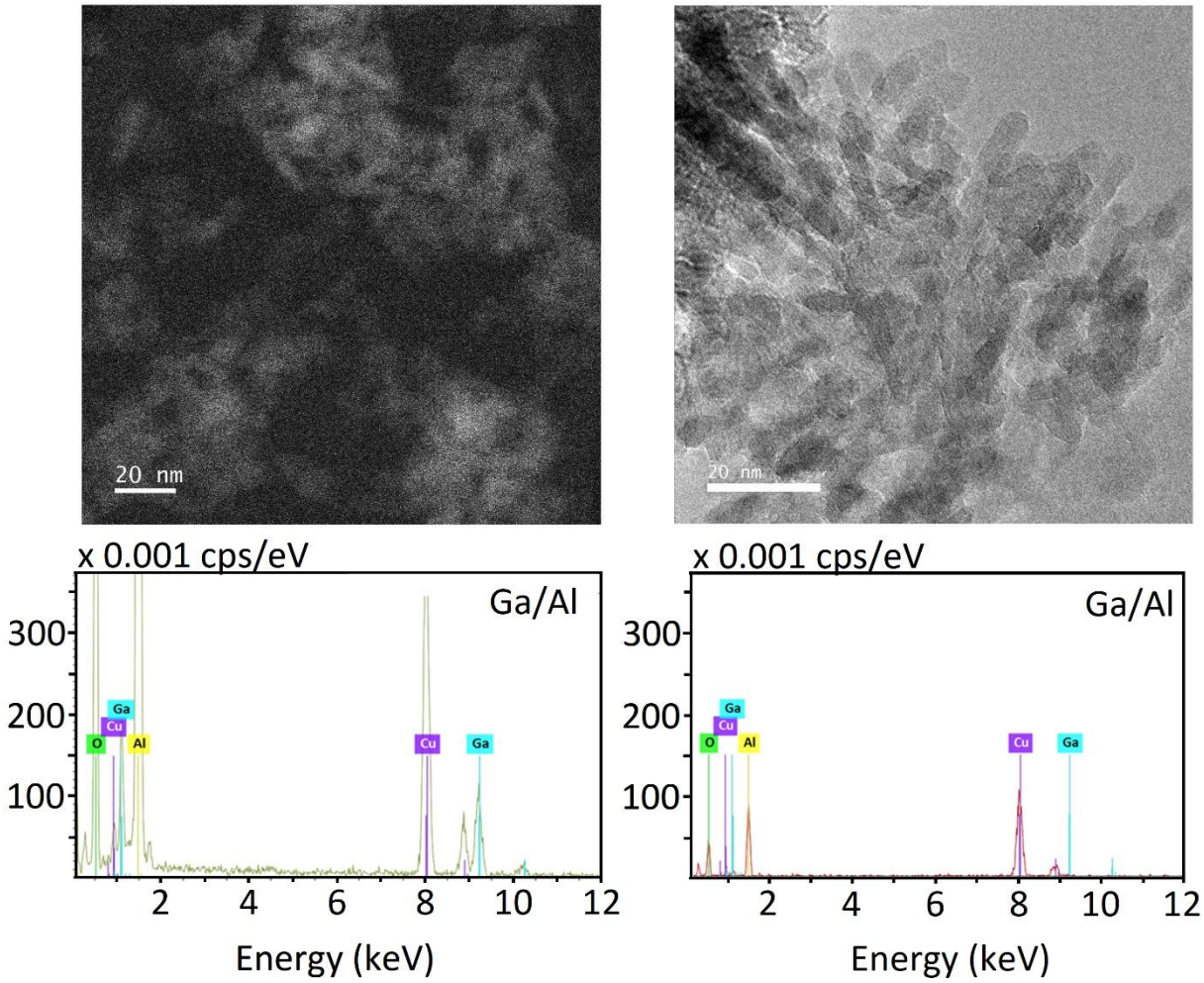

Figure S3. TEM images and EDX spectra of Ga/Al catalyst.

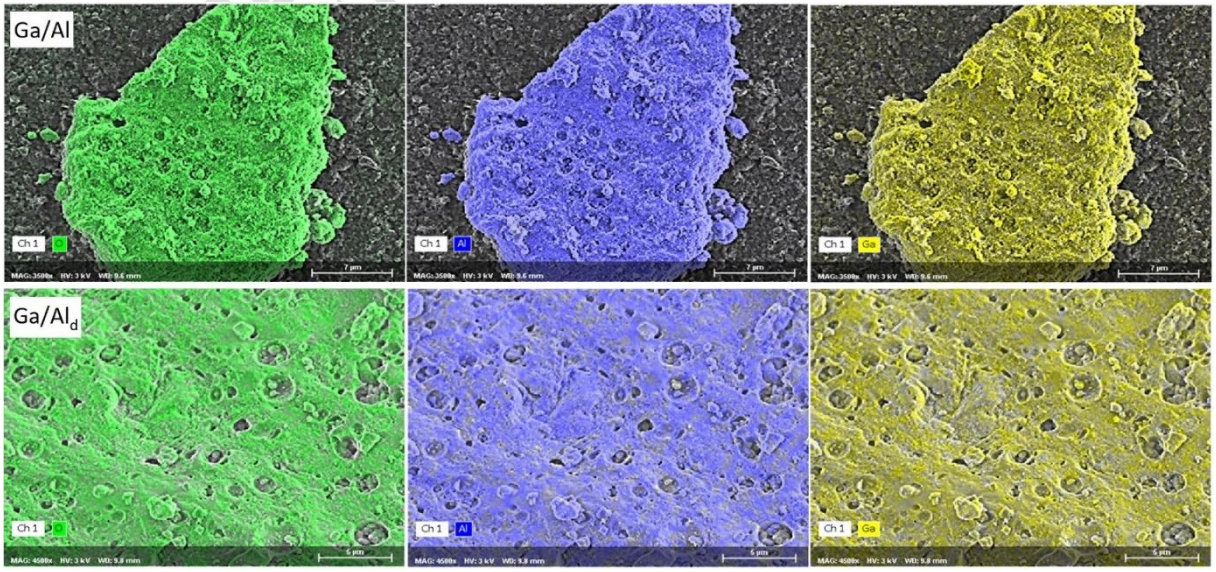

Figure S4. SEM images and EDS mapping of Ga/Al and Ga/Al_d catalysts.

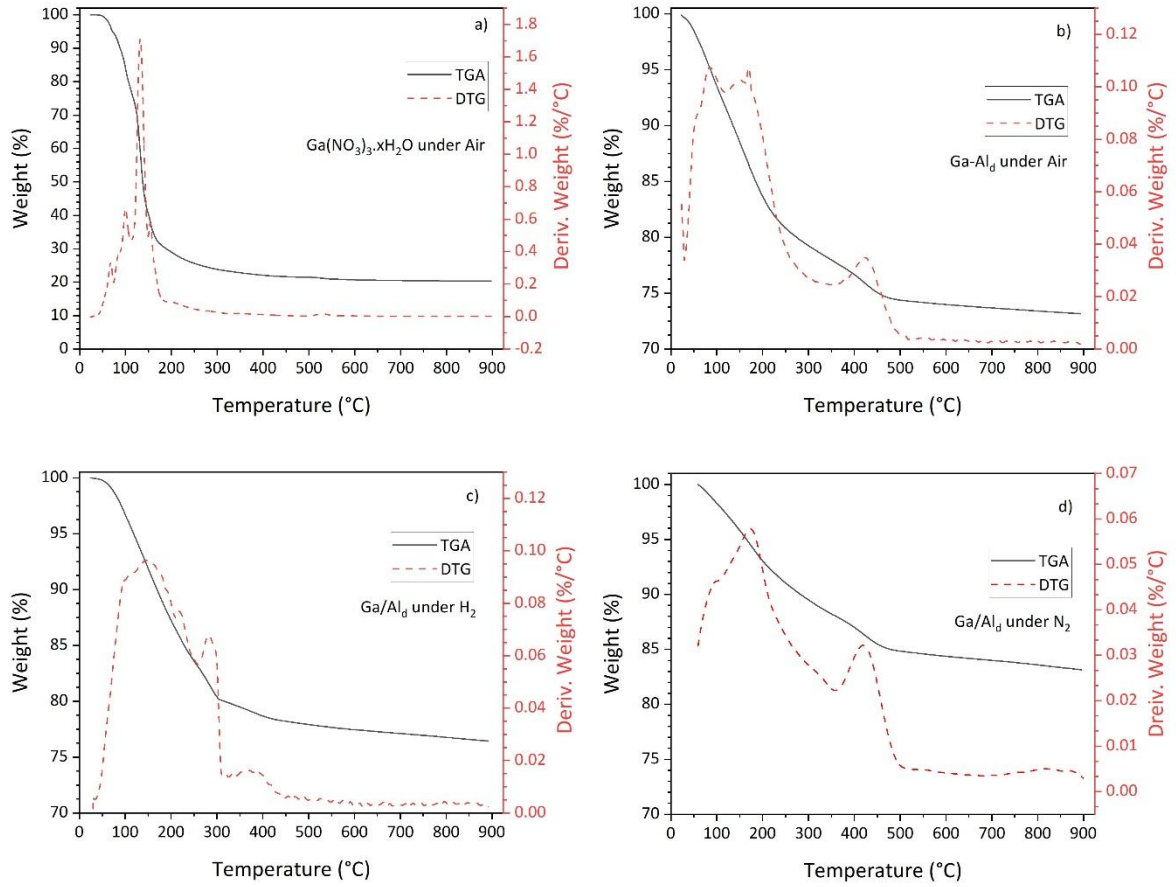

Figure S5. TGA-DTG of the (a) gallium precursor salt under air, and of Ga/Al_d catalyst during (b) calcination under air, (c) reduction under H_2, and (d) thermal decomposition under N_2. (Temperature ramp 10 °C min^{-1})

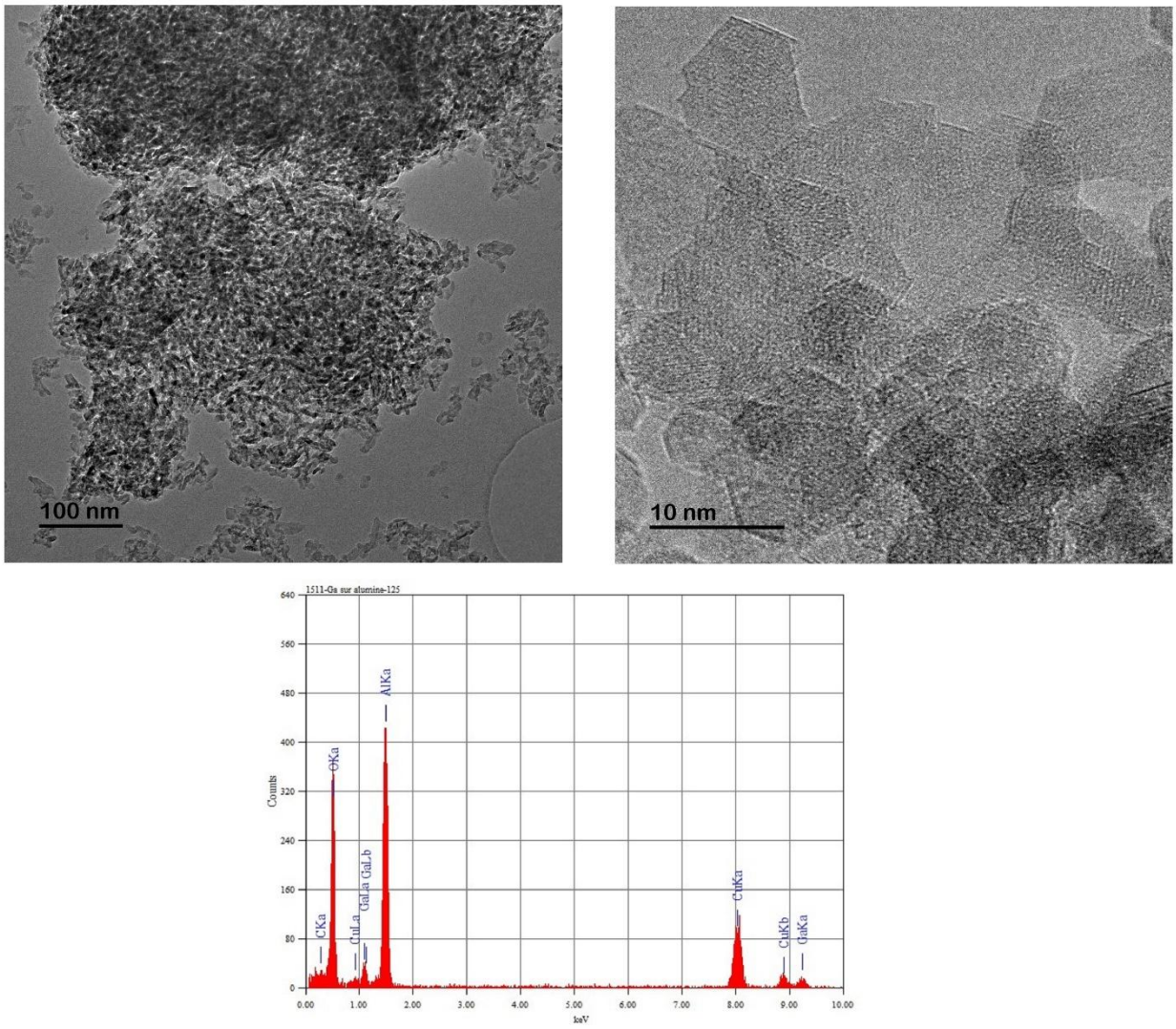

Figure S6. TEM images and EDX spectrum of Ga/Al_{red} catalyst after reduction at 650 °C under H_2 flow for 1 h (60 mL min^{-1}, 10 °C min^{-1}).

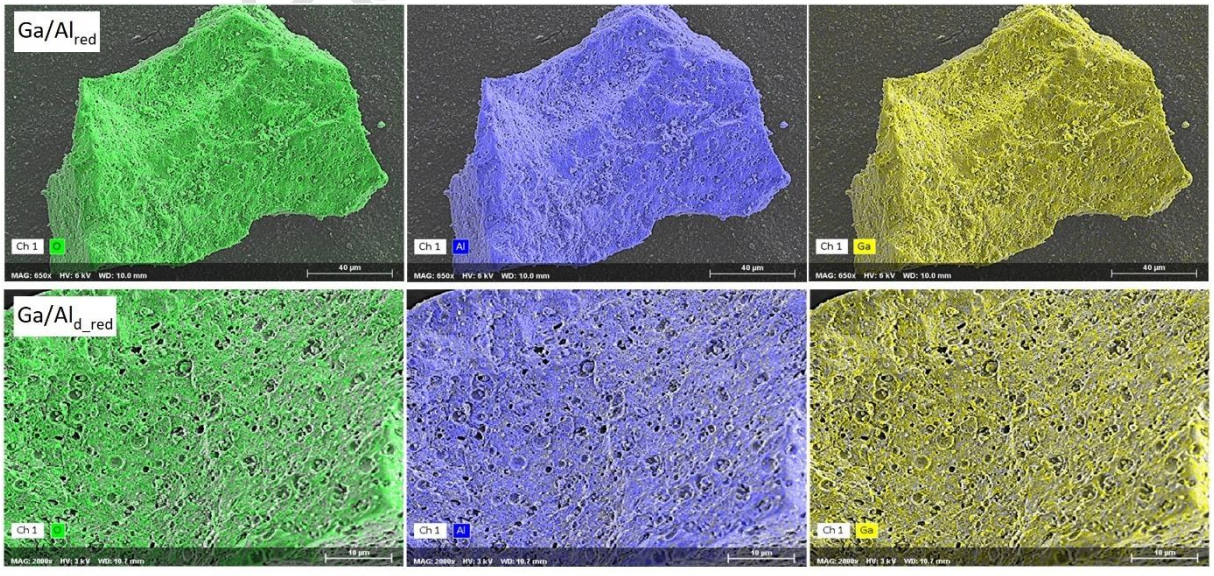

Figure S7. SEM images and EDS mapping of Ga/Al_{red} and Ga/Al_{d_red} catalysts.

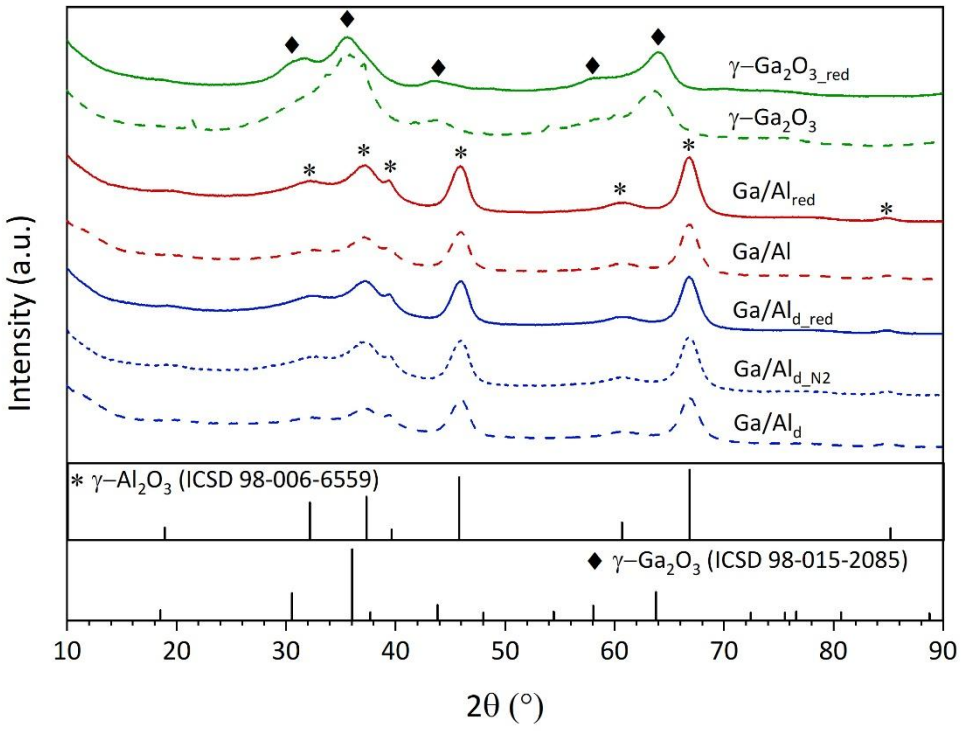

Figure S8. Effect of pretreatment on the XRD patterns of γ-Ga_2O_3, Ga/Al, Ga/Al_d catalysts: red = after reduction treatment (H_2, 60 mL min^{-1}, 1 h, 650 °C), N_2 = after treatment under N_2 at 575 °C.

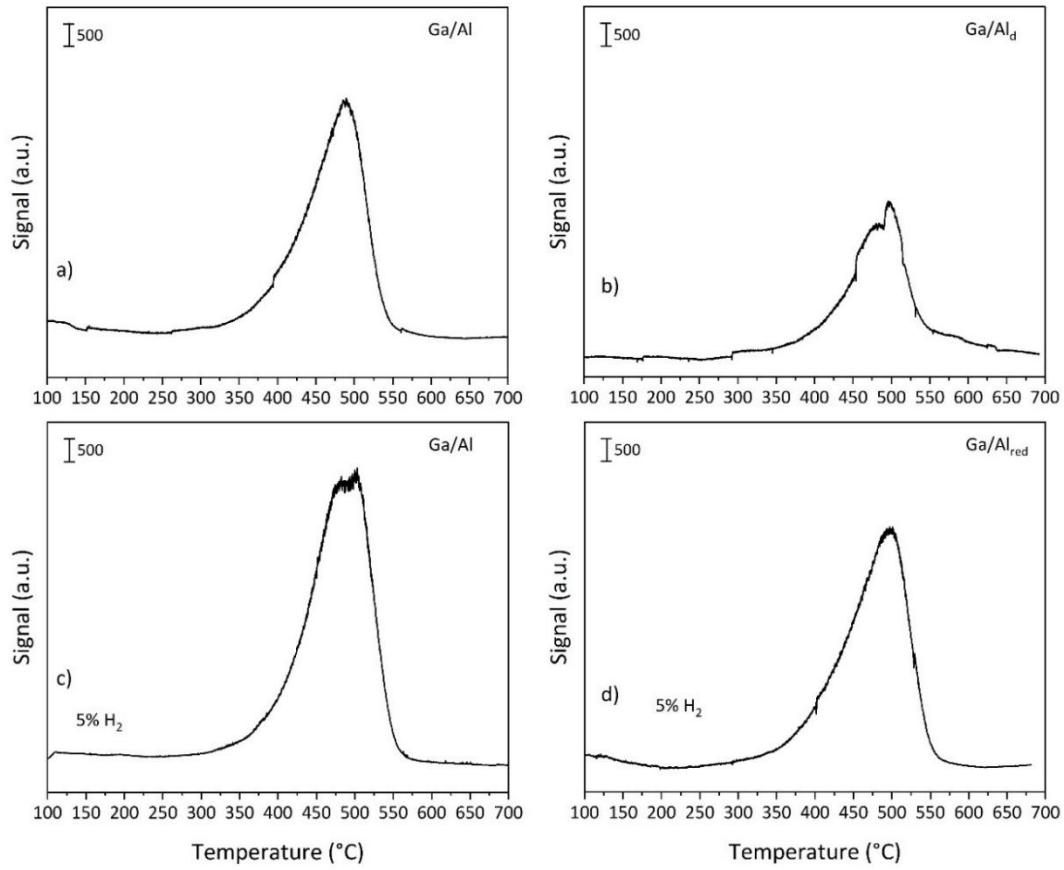

Figure S9. Temperature programmed oxidation (10 °C min^{-1}) of spent (a, c, d) Ga/Al and (b) Ga/Al_d catalysts after propane dehydrogenation at 575 °C for 4 h. Pretreatment conditions: (a, b, c) T = 575 °C, N_2, 60 mL min^{-1}, (d) T = 650 °C, H_2. Reaction conditions: T = 575 °C, WHSV = 59 h^{-1}, mass of catalysts = 100 mg, total flowrate = 100 mL min^{-1}, (a, b) $C_3H_8/N_2/H_2$ = 50/50/0, (c, d) $C_3H_8/N_2/H_2$ = 50/45/5.

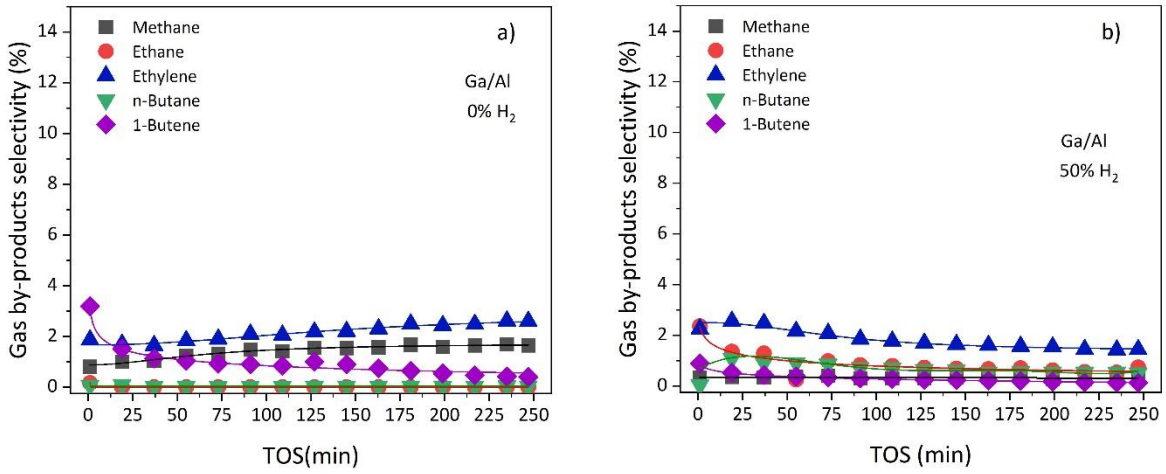

Figure S10. By-products selectivity in gas phase as a function of time-on-stream over Ga/Al catalyst under various H_2 co-feeding conditions: (a) $C_3H_8/N_2/H_2$ = 50/50/0, (b) $C_3H_8/N_2/H_2$ = 50/0/50. Pretreatment conditions: T = 575 °C, N_2, 60 mL min^{-1}. Reaction conditions: T = 575 °C, WHSV = 59 h^{-1}, total flowrate = 100 mL min^{-1}, mass of catalyst = 100 mg.

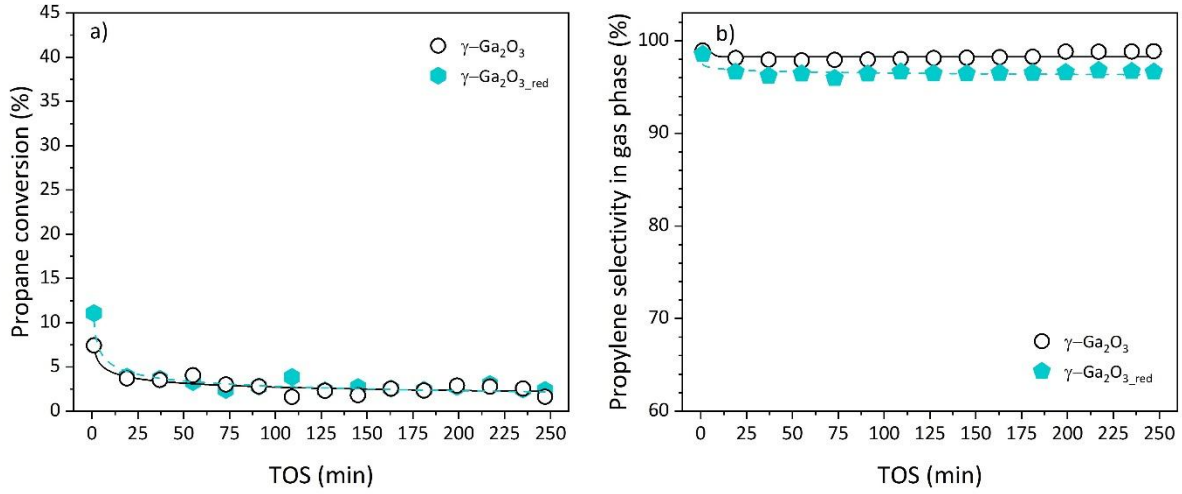

Figure S11. Evolution of (a) propane conversion, and (b) propylene selectivity in gas phase as a function of time-on-stream during PDH test over γ-Ga_2O_3 catalyst after N_2 pretreatment and without H_2 co-feeding ($C_3H_8/N_2/H_2$ = 50/50/0), and over γ-$Ga_2O_{3\_red}$ catalyst after H_2 reduction pretreatment at 650 °C for 1 h with 5 % H_2 co-feeding ($C_3H_8/N_2/H_2$ = 50/45/5). Reaction conditions: T = 575 °C, WHSV = 59 h^{-1}, total flowrate = 100 mL min^{-1}, mass of catalyst = 100 mg.

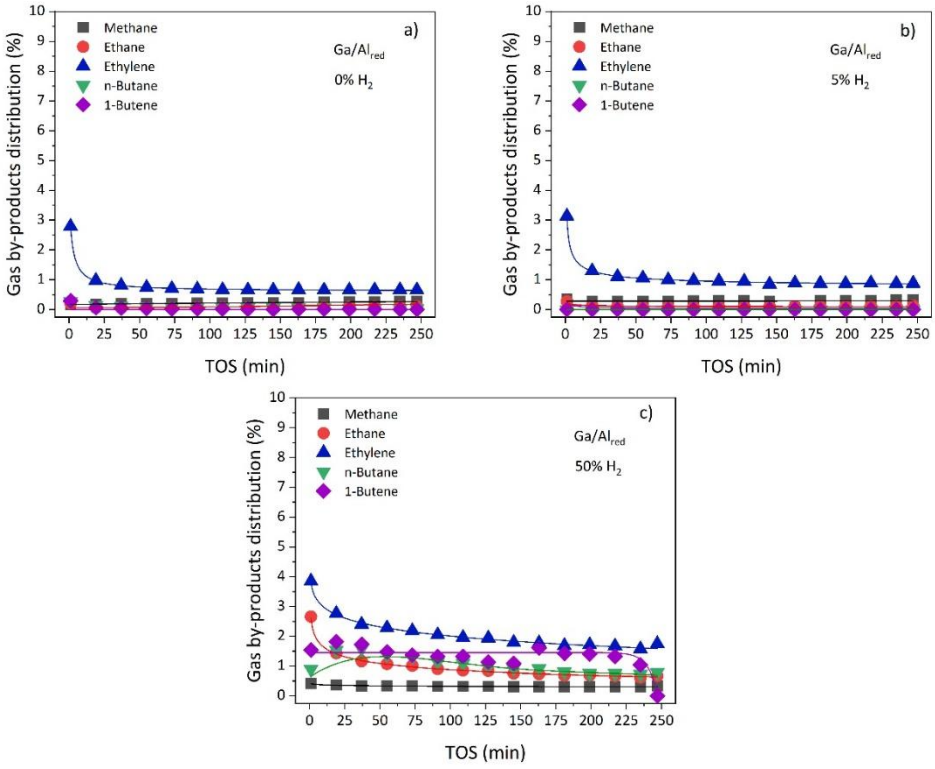

Figure S12. By-products selectivity in gas phase as a function of time-on-stream over Ga/Al_{red} catalyst under various H_2 co-feeding conditions: (a) $C_3H_8/N_2/H_2$ = 50/50/0, (b) $C_3H_8/N_2/H_2$ = 50/45/5, (c) $C_3H_8/N_2/H_2$ = 50/0/50. Pretreatment conditions: reduction at T = 650 °C under H_2 for 1 h (60 mL min^{-1}). Reaction conditions: T = 575 °C, WHSV = 59 h^{-1}, total flowrate = 100 mL min^{-1}, mass of catalyst = 100 mg.

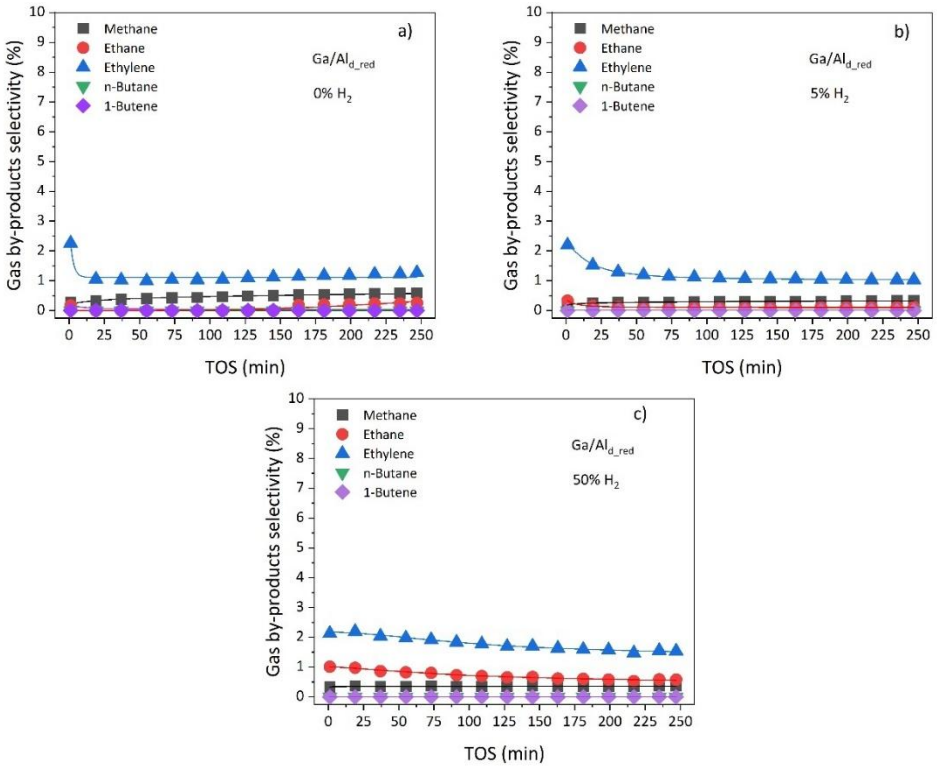

Figure S13. By-products selectivity in gas phase as a function of time-on-stream over Ga/Al$_{d_red}$ catalyst under various H_2 co-feeding conditions: (a) $C_3H_8/N_2/H_2$ = 50/50/0, (b) $C_3H_8/N_2/H_2$ = 50/45/5, (c) $C_3H_8/N_2/H_2$ = 50/0/50. Pretreatment conditions: reduction at T = 650 °C under H_2 for 1 h (60 mL min^{-1}). Reaction conditions: T = 575 °C, WHSV = 59 h^{-1}, total flowrate = 100 mL min^{-1}, mass of catalyst = 100 mg.

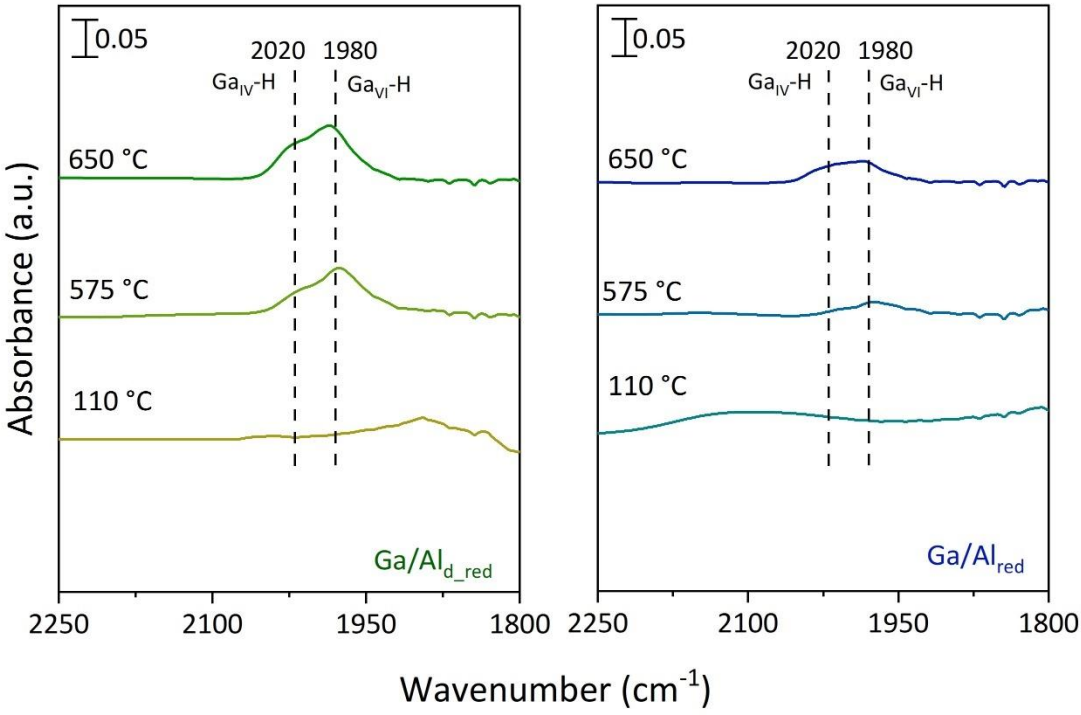

Figure S14. FTIR spectra showing the evolution of the Ga-H bands as function of reduction temperature of Ga/Al_d, and Ga/Al catalysts under H_2 pretreatment (60 mL min^{-1}, 10 °C min^{-1}).

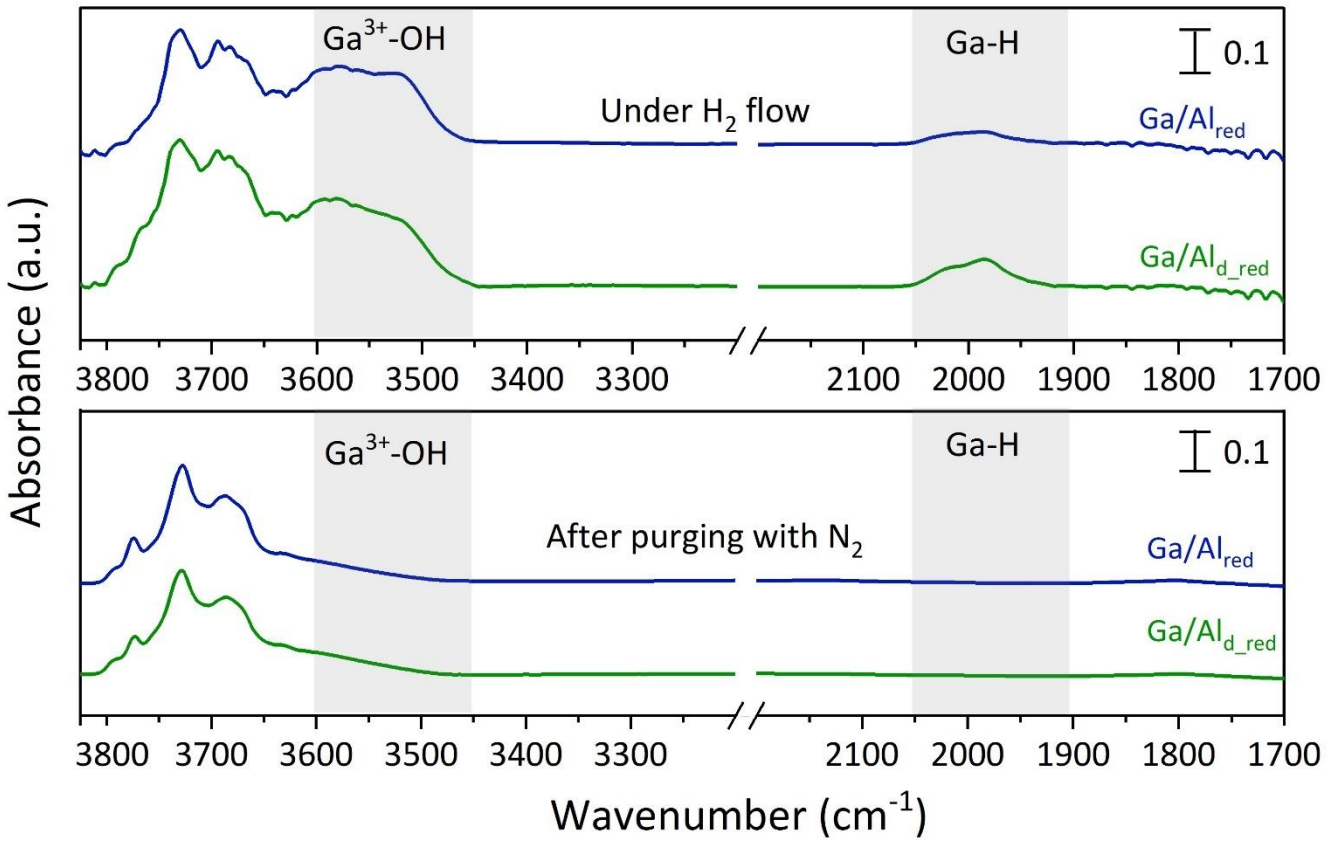

Figure S15. FTIR spectrum of gallium hydride and hydroxyl signals in the presence of flowing H_2 and then purging under N_2 at 650 °C.

Table S1. Isotropic chemical shift (δ_{iso}), quadrupolar coupling constant (C_Q), chemical shift distribution (ΔCS) and proportion of gallium environments (%) estimated from Dmfit deconvolution.

Sample	Ga_{VI}				Ga_{IV}			
	δ_{iso}	C_Q (MHz)	ΔCS	%	δ_{iso}	CQ (MHz)	ΔCS	%
Ga/Al	52.3	10.4	55	20	181.3	10.8	56	80
Ga/Al_d	60.5	12.4	45	34	184.6	11	67	66

Table S2. Isotropic chemical shift (δ_{iso}), quadrupolar coupling constant (C_Q), chemical shift distribution (ΔCS) and proportion of aluminium environments (%) estimated from Dmfit deconvolution.

Sample	Al_{VI}				A_{IV}				Al_{IV}			
	δ_{iso}	C_Q (MHz)	ΔCS	%	δ_{iso}	C_Q (MHz)	ΔCS	%	δ_{iso}	C_Q (MHz)	ΔCS	%
Ga/Al	15.1	6.02	6	69.5	--	--	--	--	74.4	6.53	10	30.5
Ga/Ald	15.1	5.87	7	63.2	38.9	6.63	6	4	74.4	6.86	10	32.8
γ-Al2O3	14.8	5.84	6	65.7	38.9	6.63	6	1.5	74.6	6.5	10	32.8

Table S3. Hydrogen consumption of γ-Ga_2O_3, Ga/Al and Ga/Al_d during the H_2-TPR until 1000 °C.

Catalyst	Temperature (°C)	H_2 consumption (µmol H_2 g_{cat}^{-1})	H_2 consumption (H_2/Ga molar ratio)
γ-Ga_2O_3	350	45	0.004
	650	4	0.00037
	> 900	-	-
	25 to 1000	***49***	***0.0044***
Ga/Al	400	17	0.024
	650	6	0.008
	930	83	0.120
	25 to 1000	***106***	***0.152***
Ga/Al_d	370	33	0.048
	650	18	0.026
	880	102	0.148
	25 to 1000	***153***	***0.222***

Table S4. Textural properties of γ-$Ga_2O_{3\_red}$, Ga/Al_{red}, Ga/Al_{d_N2} and Ga/Al_{d_red} catalysts.

Catalyst	S_{BET} (m^2 g^{-1})	V_{total} (cm^3 g^{-1})	Dp (nm)[a]
γ-$Ga_2O_{3\_red}$	104	0.13	5.0
Ga/Al_{red}	168	0.45	10.7
Ga/Al_{d_N2}	186	0.47	10.1
Ga/Al_{d_red}	107	0.40	14.9

[a] Calculated as $4V_{total}/S_{BET}$.

Table S5. Evaluation of the Brønsted acidity by the activity in the reaction of 3,3 dimethyl-but-1-ene isomerization.

Sample	Isomerization activity (mmol h^{-1} g^{-1})	$a_{rel.isom}$ (%)[a]
γ-Al_2O_3	42.31	100.0
Ga/Al	8.59	20.3

Ga/Al_d	4.48	10.6
Ga/Al_{red}	5.77	13.6
Ga/Al_{d_red}	7.63	18.0

[a] Activity of the sample divided by the one of γ-Al_2O_3 in 33DMB1 isomerization.

Table S6. Amount of GaH_x species determined by FTIR analysis under H_2 flowing for γ-$Ga_2O_{3\_red}$, γ-$Al_2O_{3\_red}$, Ga/Al_{red} and Ga/Al_{d_red}. (Pretreatment conditions: reduction at T = 650 °C under H_2 for 1 h (60 mL min^{-1})).

Catalyst	Amount of GaH_x (a.u. g_{Ga}^{-1})
γ-$Ga_2O_{3\_red}$	317
Ga/Al_{d_red}	3316
Ga/Al_{red}	1724

Table S7. Amount of GaH_x species determined by FTIR analysis as a function of the reduction temperature for Ga/Al_{red} and Ga/Al_{d_red} catalysts. (H_2 flow 60 mL min^{-1}, 10 °C min^{-1}).

Temperature of reduction (°C)	Amount of GaH_x (a.u. g_{Ga}^{-1})	
	Ga/Al_{red}	Ga/Al_{d_red}
110 °C	0	0
575 °C	881	2559
650 °C	1724	3316